NASA

Technical Memorandum **80559**

GSFC Contributions to the NATO X-Ray Astronomy Institute, Erice, July 1979

S. S. Holt and R. F. Mushotzky

SEPTEMEBER 1979

National Aeronautics and Space Administration

Goddard Space Flight Center
Greenbelt, Maryland 20771

GSFC CONTRIBUTIONS TO THE NATO X-RAY ASTRONOMY INSTITUTE, ERICE, JULY 1979

S.S. Holt and R.F. Mushotzky[1]

Laboratory for High Energy Astrophysics
NASA/Goddard Space Flight Center
Greenbelt, Maryland 20771 U.S.A.

The four lectures included in this document represent an overview of X-ray astronomical spectroscopy in general, and the results obtained by our group at Goddard Space Flight Center in particular. The lecturers gratefully acknowledge the contributions of the other group members to the development of the instruments and the interpretation of the data.

[1]Also Dept. of Physics and Astronomy, Univ. of Maryland

X-RAY SPECTRA OF SUPERNOVA REMNANTS

S.S. Holt

Laboratory for High Energy Astrophysics
NASA/Goddard Space Flight Center
Greenbelt, Maryland 20771 U.S.A.

1. X-RAY SPECTROSCOPY

Until quite recently, there has been little hard evidence for the existence of discrete features (such as emission lines) in the spectra of X-ray sources. The basic problem, of course, has been that the exposure obtainable with contemporary instrumentation has precluded the effective utilization of dispersive techniques, so that we were limited to the use of proportional counters (with typical resolving power $E/\Delta E$ no better than ~ 5) for spectroscopic study. Nevertheless, the high relative abundance of Fe has allowed the detection of both thermal and fluorescent emission lines from a variety of astrophysical contexts, even with the relatively poor resolution available with proportional counters, so that we could be certain that better resolution would eventually allow the detection of emission features from atomic transitions which were less pronounced relative to the surrounding continuum.

The model-fitting procedure we employ is a straightforward application of Poisson statistics. The raw data from an exposure to a celestial X-ray source are binned in pulse-height channels (labelled with the argument E', which should be nominally relatable to energy E); the counts accumulated in the j'th channel over the exposure are $N_j(E')$, with a Poisson error of $\delta N_j(E')$ taken to be $\sqrt{N_j(E')}$. An independent estimate of the background contributing to $N_j(E')$ over the accumulation time is $B_j(E')$, with error $\delta B_j(E')$, so that the actual "source" data accumulated are given by

$$T_j(E') = N_j(E') - B_j(E') \qquad 1.1$$

with an estimated 1σ error given by

$$\delta T_j(E') = ((\delta N_j(E'))^2 + (\delta B_j(E'))^2)^{\frac{1}{2}} \qquad 1.2$$

The only fair test of a hypothesis that a given spectral form can be adequately fitted by the data must be performed in E' (rather than E) space, because the transformation of the $T_j(E')$ to an input spectrum is non-unique. In general, the best non-dispersive spectrometers have response functions (or the probability that a photon of energy E will be recorded at a pulse-height E') with the following three characteristics:

1. A stable maximum in the response function at a pulse-height E' corresponding to E
2. A gaussian shape centered at E'-equivalent-to-E with a FWHM (= 2.36σ) such that > 50% of the response function area lies below the gaussian
3. The remainder of the response function area in a relatively featureless plateau at E' < E

More detailed discussions of the response functions of X-ray detectors may be found in the literature (e.g. Holt 1970)

The general fitting procedure begins with the assumption of a model input spectrum S(E) which is characterized by a number m of free parameters. The expectation value for the data in the j'th bin from this model is then:

$$S'_j(E') = \int_0^\infty S(E) R_j(E,E') dE \qquad 1.3$$

where $R_j(E,E')$ is the response function for the j'th channel. If there are a total of P channels for which equation 1.3 can be independently constructed, the quantity

$$\chi^2 = \sum_{j=1}^{P} \left(\frac{S'_j(E') - T_j(E')}{\delta T_j(E')} \right)^2 \qquad 1.4$$

is a suitable statistic for (p-m) degrees of freedom. Several authors have recently discussed the appropriate "acceptability" criteria to apply to overall models and to the ranges over which individual parameters can be constrained (e.g. Cash 1976). In general, the important points to remember are that there is no statistical requirement to increase the number of free parameters once an acceptable fit is obtained, and that the range of acceptable parametric values will always be model-dependent. In other words, a physically interesting set of parameters will be obtained only if a physically interesting model is chosen at the outset. Before the advent of satellite experiments, the statistical quality of the data did not permit severe constraints on potentially interesting parameters (e.g. in most cases, we found that power laws and featureless thermal bremsstrahlung continua could fit the data

equally well). More recently, we are finding that just the reverse is true (i.e. that the statistical errors are so small that most simple model forms can be excluded, and that our ability to achieve statistically adequate fits is limited by the availability of detailed model calculations).

All of the data presented in this lecture will be analyzed in this manner, but it is worth discussing alternative data presentations which appear in the literature. Because the above approach is model-dependent, a simple model-independent manner in which the ordinate of a figure labelled "counts" can be converted into "incident photons" is to construct

$$S^{(n+1)}(E) = \frac{T_j(E')\, S^{(n)}(E)}{\int_0^\infty R(E,E')S^{(n)}(E)\, dE} \qquad 1.5$$

where the superscripts on the input spectra refer to the trial number. If, for the initial guess at a trial spectrum, a flat spectrum $S^{(1)}(E)$ = constant is used, it is clear that subsequent iterations are likely to yield a convergent value of $S^{(\infty)}(E)$ which is independent of any a priori assumptions about the input spectrum. A χ^2-test of $S^{(\infty)}(E)$ against trial models in E-space may then be performed, but it is not quite as sensitive as that of equation 1.4 because the iteration process tends to smooth out sharp features which might be present in the true input spectrum.

A representation for the input spectrum which is quite popular at present replaces $S^{(n)}(E)$ in equation 1.5 with the input spectrum deduced from the fitting procedure in E'-space. The difficulty with this representation is that the model-independency has been removed, so that sharp features which may be incorrectly introduced into the fitting procedure will be enhanced in the data presentation. Much of the recent proportional counter data in the literature has been displayed in this manner. A new technique developed by Blissett and Cruise (1979) appears to offer the best features of both (i.e. model independency and enhancement of treal features). In this approach, the data are essentially filtered with a window function commensurate with the resolution of the detector, so that only those sharp features which are at least as wide as the natural detector response in E'-space will survive the spectral inversion.

2. DIFFUSE X-RAY PRODUCTION

The simplest model spectra are expected from those astrophysical situations for which X-ray transfer effects in the source are minimized. Such "diffuse" X-ray sources can be generally characterized by single interactions of electrons with electromagnetic fields which give rise to X-ray emission. If we assume that the

electrons of interest can be approximately represented by a power law spectrum:

$$\frac{d^2N}{dVd\gamma} \propto \gamma^{-\Gamma} \text{ cm}^{-3} \qquad 2.1$$

where γ is the electron Lorentz factor, the rate at which the electron loses energy in interactions with the field is

$$-\frac{d\gamma}{dt} = \frac{4}{3}\frac{\sigma_o}{mc}\rho\,\gamma^2 \quad \text{s}^{-1} \qquad 2.2$$

where ρ_o is the Thomson cross-section and ρ is the energy density in the field. The characteristic "cooling time" of the process is then simply

$$\tau = \left(\frac{1}{\gamma}\frac{d\gamma}{dt}\right)^{-1} = \frac{3mc}{4\sigma_o}\rho\gamma \quad \text{s} \qquad 2.3$$

In the case of Compton interactions, the field energy density is that in soft target photons (e.g. infa-red or optical). For synchrotron radiation, the appropriate energy density is that in the magnetic field, $B^2/8\pi$. Coulomb collisions can also be formally accommodated by equations 2.2 and 2.3, but the fact that the X-ray yield is so low ($\sim 10^{-4}$) means that the appropriate distribution of electrons to consider is not a power law, but is instead an equilibrium Maxwellian to reflect the fact that a large number of Coulomb collisions are required in order to produce an X-ray photon. The two non-thermal processes yield power-law X-ray spectra with energy index $\alpha = (\Gamma-1)/2$, where Γ is the spectral index from equation 2.1 in the energy range appropriate to the electrons responsible for the X-ray production. The X-radiation produced by Coulomb interactions has an equilibrium spectral form given by

$$E\frac{dq}{dE} \approx 10^{-19}\, g\, Z^2 n^2\, (kT)^{-\frac{1}{2}}\, e^{-E/kT} \quad \text{erg cm}^{-3}\,\text{erg}^{-1} \qquad 2.4$$

The expression in equation 2.4 is the volume emissivity for bremsstrahlung only, and any line emission must be added to it in order to determine the total X-ray emission; above $\sim 10^7$ K bremsstrahlung dominates, while line emission dominates the cooling at lower temperatures. T is the temperature, k is the Boltzmann constant, n is the density, Z is the effective atomic number of the plasma (~ 1.3 for cosmic abundance) and g is the Gaunt factor which, for temperatures in our range of interest, can be approximated by

$$g \approx (E/kT)^{-0.4} \qquad 2.5$$

The total bremsstrahlung luminosity per unit volume can be obtained by integrating equation 2.4 over energy, so that an effective cooling time can be defined as the ratio of the plasma kinetic energy density to the luminosity per unit volume:

$$\tau \approx 10^{19} \frac{\sqrt{kT}}{n} \quad s. \qquad 2.6$$

It is important to note that the bremsstrahlung X-rays are produced by electrons of comparable energy, while the non-thermal processes typically require electrons of much higher energy. For Compton interactions, an X-ray of energy E will result from a single scattering of a photon of initial energy E_o according to

$$\langle E \rangle = \frac{4}{3} \gamma^2 \langle E_o \rangle \qquad 2.7$$

while the analogous synchrotron case (in a field of magnitude B) will be

$$\langle E \rangle \approx 10^{-20} \gamma^2 B \quad \text{ergs} \qquad 2.8$$

The production of 10 keV photons from 1 eV photons or a 1 gauss field would require, therefore, γ of 10^2 or 10^6, respectively. More detailed treatments of diffuse X-ray production may be found in many references (e.g. Blumenthal and Tucker 1974; Holt 1974).

3. X-RAY PRODUCTION IN SUPERNOVA REMNANTS

The prime examples of diffuse X-ray production in galactic X-ray sources are the X-ray emitting supernova remnants. The energy source in these remnants is the kinetic energy which still remains from the initial supernova outburst.

The Crab nebula is a special case, in the sense that we have yet to find another remnant with the same X-ray characteristics. It contains a pulsar (i.e. a rotating magnetized neutron star) which rotates with a period of 33ms. The fact that the pulsar is slowing down with time was one of the pieces of evidence which originally led to its identification with a neutron star; its importance in the present context is that the rate at which it is losing rotational kinetic energy matches the total luminosity of the remnant in all energy bands. Pacini pointed out that since the rate at which energy is converted to electromagnetic modes scales like P^{-4} (P is the rotation period), and pulsed X-ray luminosity created at the speed-of-light-circle scales like P^{-10}, it would be unlikely that other remnants would be found which could either power X-ray sources at a level > 10^{36} ergs/s, or

which would yield X-ray pulsations; in particular, the next-fastest rotator, that in Vela X with a period of 87 ms, does neither. It is important to note that "pulsars" are defined here as those neutron stars whose rotational energy is responsible for radio or X-ray luminosity; "X-ray pulsars" in binary systems derive their energy from other means, as will be discussed in later lectures.

We are now certain that the X-radiation from the Crab nebula remnant arises from synchrotron emission. The spectrum is well-fit by a power law out to at least 100 keV (e.g. Dolan et al. 1977) and Weisskopf et al. (1976) have measured X-ray polarization which matches that in the optical. There remain some difficulties in the theoretical considerations involved in applying the appropriate electrodynamics to efficiently transfer the rotational energy to X-ray production in detail, but both the energy source (rotational kinetic energy) and the final X-ray production mechanism (synchrotron radiation) are firmly established.

The other SNR which are X-ray emitters are quite different in all observational respects. There is no evidence whatsoever for pulsars at their centers, but we still believe that they are powered by kinetic energy; in these cases, the kinetic energy is that contained in the ejecta originally expelled by the explosion. The traditional theory of Shklovsky (1968) was first investigated in detail by Heiles (1964) for its X-ray implications, and many newer treatments may be found in the literature (e.g. Itoh 1977).

In bare outline, the post-explosive history of supernovae may be characterized by three distinct phases. In the first phase, the ejecta move supersonically out through the interstellar medium, with the attendant shock accumulating ISM material (but not so much as to effectively brake the outflow, i.e. the SNR radius increases linearly with time). When the accumulated mass becomes comparable to ejected mass, the shock slows down because of its increased inertia. It is during this phase that X-ray emission becomes important, because of both the increased mass and the lower temperatures associated with the decreasing shock velocity. When X-ray cooling becomes so large that the expanding remnant loses a significant fraction of its energy, it rapidly slows down (the third phase) and eventually breaks up into the ISM.

The second phase is often called the "adiabatic" phase because the X-ray cooling is not yet high enough to have radiated away a substantial fraction of the initial energy, and the Sedov similarity solution yields the following relations. The remnant radius R, in terms of the initial energy of the ejecta ϵ_o, the ISM mass density in front of the shock ρ_o and the age of the remnant t is

$$R \approx \left(\frac{\epsilon_o}{\rho_o}\right)^{1/5} t^{2/5} \approx \frac{5}{2} V t \qquad 3.1$$

where V is the present shock velocity. The temperature T of the material which has equilibrated with the shock is

$$T \approx \frac{3}{16} \frac{\bar{m}}{k} V^2 \approx 2 \times 10^{-9} V^2 \qquad 3.2$$

where $\bar{m}$ is the mean ion mass. The density just behind the shock is four times that in the unshocked ISM, and Heiles estimates the total volume emission measure of the shell to be

$$n^2 V \approx 10\, n_o^2 R^3 \qquad 3.3$$

where n_o is the number density in the ISM. The Crab will probably never be such a thermal "shell" source because the ISM density in its neighborhood is so low that such a snowplow will never be effective there. Many other remnants do exhibit this type of behavior, however, as we shall see below. It is important to note that as the X-ray luminosity of a shell source increases, we expect its temperature and shell velocity to decrease, so that it cools more even more rapidly as it progresses toward the third phase.

4. X-RAY SPECTRA OF SUPERNOVA REMNANTS

Even before the launch of Einstein, several supernova remnants were known to be thermal sources not just because they could be fit with bremsstrahlung continua, but also because thermal Fe emission at 6.7 keV could be unambiguously detected with proportional counters. Surprisingly, the temperatures to which the continua could be fit were considerably lower (several keV rather than several tens of keV) than that prescribed by equation 3.2 on the basis of the observed shock velocities, at least in the cases of Cas A and Tycho, and the fits further required the addition of lower temperature components to match the data below $\sim$ 4 keV. Even in the case of Fe K-emission, where the line is well separated from others and the continuum is falling rapidly so that the equivalent continuum width exceeds 1 keV, the emission feature appears only as a discontinuity in the smooth continuum rather than a sharply defined emission line. For the emission lines expected below 4 keV from lower-Z components, there is no hint of structure in the raw data from proportional counters.

The Einstein Observatory contains a variety of dispersive and non-dispersive spectroscopic tools for the investigation of celestial X-ray sources. I will describe, here, some results from the solid-state-spectrometer (SSS), a non-dispersive device which combines high efficiency with resolution sufficient to separate individual line components, although they cannot be completely resolved. Figure 1 illustrates the capability of separating expected line features with the $\sim$ 160 eV FWHM resolution of the instrument. Not only can individual elements be easily separated, but hydrogen-like, helium-like and neutral fluorescence lines from the same elements can be separated, as well. The total field-of-view of the SSS is approximately 6 arc-minutes in diameter, and

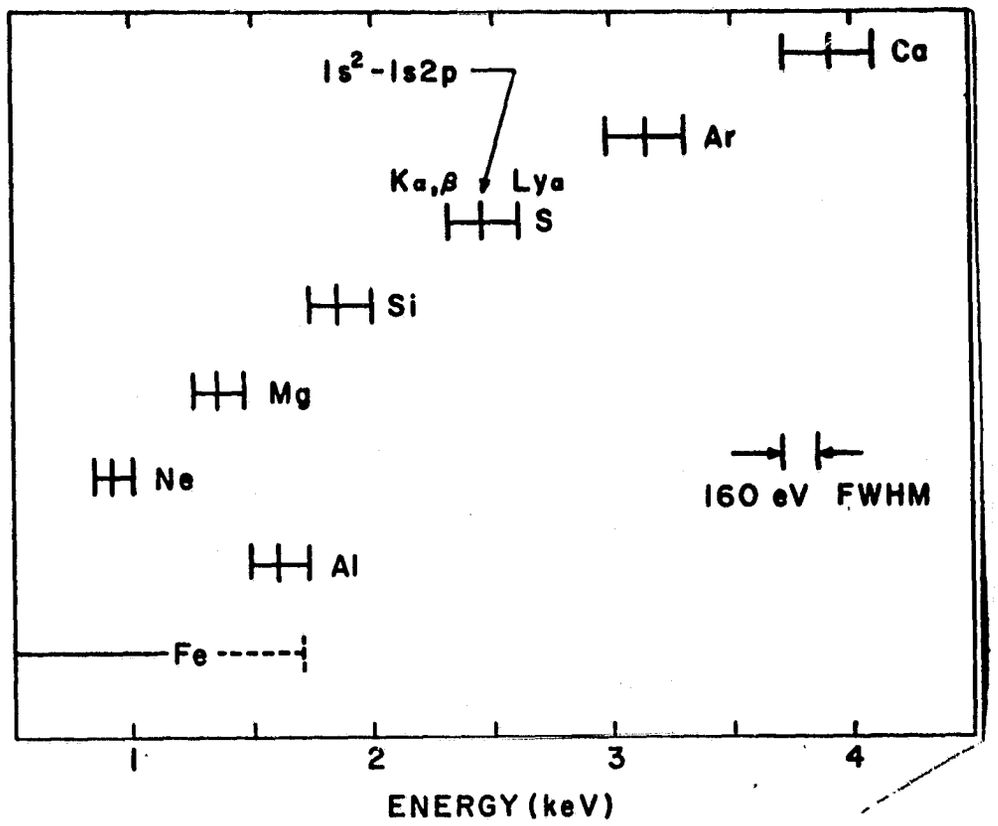

Fig. 1. Comparison of the Einstein SSS energy resolution with the separation between line features which might be expected to be prominent in X-ray sources.

its effective energy range is 0.8 - 4.5 keV. Additional instrumental details may be found in Joyce et al. (1978) and Holt et al. (1979).

A sample of the spectra obtained with the SSS from supernova remnants is shown in Figure 2. The data displayed are all raw pulse-height counts, compared with a solid histogram representing a model fit, as described in Section 1. The Crab nebula is fit with a power law only, and the others are fit with two-temperature thermal spectra. In the latter cases, the dashed lines represents the total contributions from elements with atomic number $\leq$ 10 (i.e. the large fraction of the continuum). For Cas A, where the exposure is greatest, there is statistical significance associated with line emission from Fe L-transitions, as well as from K-transitions of Mg, Al, Si, S, Ar and Ca; furthermore, both helium-like and hydrogen-like components are observed from Si and S (although the former are at least an order of magnitude more prominent). For Tycho, where the peak of the Si line is more than an order of magnitude above the continuum, fully 50% of the photons detected are in the Si and S lines.

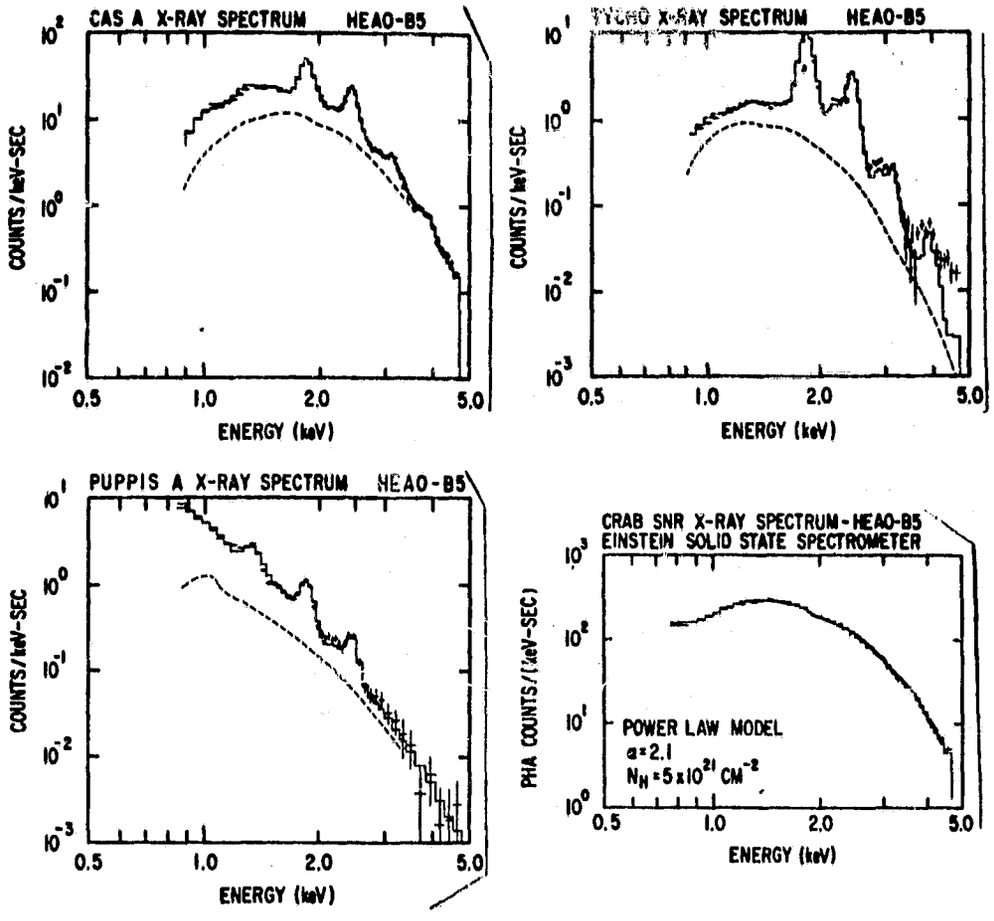

Fig. 2. Einstein SSS experimental spectra of four supernova remnants.

All of the spectral fits for the displayed thermal spectra (and those of similar remnants not explicitly displayed in Figure 2) are performed in the same manner. A high temperature component is fixed from previously obtained HEAO A-2 data, and we allow a lower temperature component, the abundances of all the line-prominent elements, and the relative normalizations of the two temperature components to be free parameters (the same abundances for both components). The models assume that the two components are each separately in collisional equilibrium (Raymond and Smith 1977,1979).

5. DISCUSSION OF SPECTRAL RESULTS

The younger remnants (Cas A, Tycho and Kepler are all $\sim$ 400 years old) display spectra with marked similarities. The abundances,

in particular, exhibit the following peculiarities: Fe and Mg are slightly less than solar, but Si, S and Ar are each in excess of solar and appear to go in the ratio 1:2:4. The Si abundance in both Cas A and Kepler is approximately twice solar, while that in Tycho is approximately seven times solar. The obvious problem with these "abundances" is that they are intimately connected with the model assumptions. In particular, they are based on the assumptions that the abundances of all the $Z \leq 10$ elements are in solar proportions, and that the two thermal components are in collisional equilibrium. We have no way of directly measuring the validity of the former, and we are painfully aware that the latter is not expected to be true for a recently shock-heated plasma.

Pravdo and Smith (1979) have recently concluded, on the basis of detailed interrogation of HEAO A-2 data for Cas A and Tycho, that the "high temperature component" shows evidence of extending all the way from the few keV which constitutes the "best fit" to the much higher temperatures predicted from equation 3.2. This component is clearly not in equilibrium, but its precise modelling affects the overall abundances through the true contributions to the high ionization state lines and the continuum. The lower temperature component (typically, 0.5 - 0.6 keV for these young remnants) is probably characteristic of material which is cooling behind the shock, and may be closer to an equilibrium configuration. It is probably true, therefore, that the Si and S abundances we fit are probably the closest to being correct (consistent with a solar lower-Z elemental distribution), since they are so prominent. The Ar abundance is more affected by the high temperature continuum, the Fe is sensitive to the temperature distribution, and the Mg is coupled to the Fe because the L-lines from the latter confuse the continuum near the K-lines from the former.

Nevertheless, there are some consistent trends which are evident in the young SNR spectra. Even though the emitting plasma is an unknown mixture of ejecta, swept-up ISM and pre-explosive stellar mass loss, there is a clear overabundance of Si-group material relative to Fe, as in the fast-moving optical filaments of Cas A (Kirshner and Chevalier 1977). This relative overabundance is approximately the same in Kepler (Type I) and Cas A (Type II), while Tycho (Type I) is about a factor of four higher. This suggests that the pregenitor for Type I SNR is a relatively low mass star (Tinsley 1979) rather than the He star for which Arnett (1979) has calculated pronounced overabundances in the Fe-group ejecta. The approximately solar Fe abundances deduced from the Fe-L blends are in agreement with the Fe-K intensities previously measured in earlier experiments.

Older remnants (e.g. Puppis A), which are $> 10^3$ years old and have radii > 10 pc, seem to exhibit very consistent abundances in all line-prominent elements. The ionization temperatures deduced from the best fits are only slightly less than those for the younger remnants, and we are presumably measuring a near-equilibrium situation with abundances which should be approaching

solar. In fact, the best-fits require abundances which are approximately twice solar for all elements except S, for which the abundance is twice as high. There is a strong suggestion from both the older and younger SNR (as well as from the spectra measured from other thermal sources not discussed in this lecture) that the relative abundance of S called "solar" by Raymond and Smith is about a factor of two low, i.e. that the actual solar abundance of S relative to Si is a factor of two higher.

Remnants which are even older, such as Cyg Loop, are too cool to be observed with the SSS. Cyg Loop is undoubtedly cooling very rapidly via line emission (unfortunately, the oxygen emission is below the SSS threshold), and the remnant is entering the third (and last) phase of significant X-ray production and SNR morphology.

Clearly, the obvious next step in the understanding of the spectral data from SNR requires detailed modelling of the hydrodynamics and ionization balance in order to convert the apparent abundances to true abundances. The imaging data obtained from Einstein will be crucial to the construction of detailed models, and the constraints imposed by both the imagery and the spectroscopy should remove a large fraction of the non-uniqueness which has characterized such modelling in the past.

REFERENCES

Arnett, W.D., 1979, Ap. J. (Letters) 230, L37.
Blissett, R. and Cruise, A.M., 1979, MNRAS 186, 45.
Blumenthal, G.R. and Tucker, W.H., 1974, in X-Ray Astronomy (D. Reidel Publishing Company, Dordrecht-Holland).
Cash, W., 1976, Astr. Ap. 52, 307.
Dolan, J.F., Crannell, C.J., Dennis, B.R., Frost, K.J., Maurer, G.S., and Orwig, L.E., 1977, Ap. J. 217, 809.
Heiles, C., 1964, Ap. J. 140, 470.
Holt, S.S., 1979, in Introduction to Experimental Techniques in High Energy Astrophysics, NASA SP-243, 63.
Holt, S.S., 1974, in High Energy Particles and Quanta in Astrophysics (MIT Press, Cambridge, Massachusetts).
Holt, S.S., White, N.E., Becker, R.H., Boldt, E.A., Mushotzky, R.F., Serlemitsos, P.J., and Smith, B.W., 1979, Ap. J. (Letters), in press.
Itoh, H., 1977, Publ. Astron. Soc. Japan 29, 813.
Joyce, R.M., Becker, R.H., Birsa, F.B., Holt, S.S. and Noordzy, M.P., 1978, IEEE Trans. Nucl. Sci. NS-25, 453.
Kirshner, R.P. and Chevalier, R.A., 1977, Ap. J. 218, 142.
Pravdo, S.H. and Smith, B.W., 1979, Ap. J. (Letters), in press.
Raymond, J.C. and Smith, B.W., 1977, Ap. J. Suppl. 35, 419.
Raymond, J.C. and Smith, B.W., 1979, in preparation.
Shklovsky, I.S., 1968, Supernova (Wiley, New York).
Tinsley, B., 1979, Ap. J. 229, 990.
Weisskopf, M.C., Cohen, G.G., Kestenbaum, H.L., Long, K.S., Novick, R., and Wolff, R.S., 1976, Ap. J. (Letters) 208, L125.

X-RAY SPECTRA OF GALACTIC X-RAY SOURCES

S.S. Holt

Laboratory for High Energy Astrophysics
NASA/Goddard Space Flight Center
Greenbelt, Maryland 20771 U.S.A.

1. BINARY X-RAY SOURCES

With the exception of a few supernova remnants, we presently believe that all the X-ray sources in the galaxy with $L_X \gtrsim L_\odot$ arise in binary systems, one member of which is a degenerate dwarf, a neutron star, or a black hole. The energy source for the x-radiation in such a system is the gravitational energy liberated when mass is transferred to the surface of the degenerate star, i.e.

$$L_X = \eta G \frac{\dot{M}_X M_X}{R_X} \qquad 1.1$$

where R_X and M_X are the radius and mass of the compact X-ray star, $\dot{M}_X$ is the rate at which mass is accreting onto the object, and η is the efficiency with which this gravitational potential energy may be converted to X-rays (a typical value might be ~ 0.1). The requirement that the star be compact is an obvious consequence of the total gravitational potential energy liberated by a proton falling from infinity to the surface of a 1 $M_\odot$ star:

$$G \frac{m_p M_\odot}{R_X} \approx 2 \frac{R_\odot}{R_X} \quad \text{keV} \qquad 1.2$$

Since the radiation yield in bremsstrahlung is so low, it is clear that we must have $R_X << R_\odot$ for efficient X-ray production. A typical white dwarf radius of 10^8 cm will yield $\sim$ 1 MeV in equation 1.2, and a neutron star will yield 100 times more.

Of the catalogued varieties of binary X-ray sources, we are

certain that white dwarfs are the compact objects in cataclysmic variables, and that neutron stars are present in the X-ray "pulsars". Note that the latter objects have unfortunately been given the same name as the central source in the Crab nebula; it is true that both types are rotating magnetic neutron stars, but those in binary systems are actually acquiring rotational kinetic energy rather than expending it. There are many other historic classifications of sources (e.g. "soft" transients, bursters, bulge sources, halo sources) for which arguments have been made for both dwarf and neutron star compact objects, with the latter generally being favored. In addition, at least three objects (Cyg X-1, Cir X-1 and V861 Sco) have been tentatively identified with black holes. Of these, the strongest case can apparently be made for Cyg X-1, where a compact object with a mass which exceeds that possible for either a neutron star or a white dwarf seems to be required. The argument for Cir X-1 is circumstantial, and based on similarities in short-term temporal variations with Cyg X-1. The case for V861 Sco now appears to have been based on a misidentification.

The remainder of this lecture will be devoted to the spectroscopic properties of broad classes of galactic sources, and will not substantially address the very basic evolutionary considerations which a detailed description of these objects requires. The reader is directed to the lectures of Prof. van den Heuvel in this volume for an excellent review of the elements of our present understanding of the fundamental nature of binary X-ray sources.

Spectroscopically, the prime a priori characteristic which distinguishes galactic binaries from the diffuse sources discussed in previous lectures is that the photon transport in the source can no longer be ignored. In the cases of supernova remnants and clusters of galaxies, the assumption of direct transmittal of the X-ray photons to our detectors, with only the interstellar medium intervening, was a good one. Here, however, the X-ray photons are liable to suffer a considerable number of inelastic collisions before escaping the source region, so that we do not expect to be able to measure the production spectrum directly.

In most accretion scenarios, the infalling material cannot fall directly to the surface of the compact star because of the angular momentum that it carries. The material must, therefore, spiral into the star, so that the probability of an accretion disk forming around the object is quite high (e.g. Pringle and Rees 1972). X-radiation produced by viscosity in the disk will be multi-temperature as it will arise from differing disk positions, and the optical depth for Thomson scattering will be $\gg 1$. Even if the emission comes from close to the stellar surface (as we might expect near the magnetic poles of X-ray pulsars), obscuration by material in the disk or at the Alven surface will almost certainly result in high Thomson optical depths for most geometries. In fact, the very condition which limits the luminosity of compact X-ray sources, the Eddington condition

$$L_x \lesssim 10^{38} \frac{M_x}{M_\odot} \qquad 1.3$$

is that imposed by the balance of the gravitational and radiation pressures on the infalling material, where the latter is dominated by Thomson scattering.

In summary, the same compactness which allows binary sources to be powerful X-ray sources often prevents the direct observation of the initially produced X-radiation via electron scattering in the source region itself. Emission signatures (such as thermal emission lines) will, therefore, be largely washed out by the transport of the photons out of the source. A large number of treatments of this scattering have appeared in the literature, the most recent (and complete) being that of Sunyaev and Titarchuk (1979). Typically, smooth power-law spectra are expected over limited dynamic ranges, with the indices determined primarily from the Thomson optical depth and the scattering electron temperature, and only secondarily from the input X-ray spectrum if the scattering depth is high enough.

2. CATACLYSMIC VARIABLES

These binary systems, with a white dwarf as the compact object, include the recurrent and classical novae as well as the "polar" systems such as AM Her. They suffer much less from Thomson scattering than most other binary X-ray sources, possibly because they radiate considerably below their Eddington-limited luminosities. They possess accretion disks from which most of the optical variation is observed (particularly that associated with the "hot spot" where the accreting material is channelled into the disk), but the disk temperatures are much too cool to be responsible for the X-ray emission. The X-rays are presumed to arise from material which is directly falling to the stellar surface. Fabian, Pringle and Rees (1976) have calculated that effective X-ray temperatures of $\sim 10^8$ K should be observed from material which is being spherically accreted onto white dwarfs, and the spectra of cataclysmic variables observed with proportional counter experiments onboard OSO-8 and HEAO-2 have detected such thermal components from Am Her, U Gem, SS Cygni and EX Hydrae. It is important to note that AM Her (which has the highest X-ray temperature of the four) is the only one for which direct evidence for X-ray production at the dwarf stellar surface exists. The hard AM Her X-rays exhibit modulation consistent with self-eclipsing of the magnetic poles, with subsequent reflection and fluorescence from adjacent regions. The others are completely consistent with optically thin bremsstrahlung spectra, and the presumption of spherical accretion is based only upon consistency with the observed temperature.

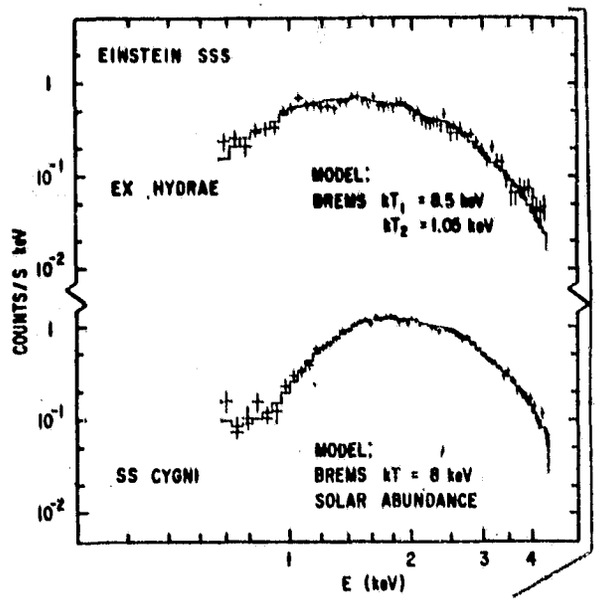

Fig. 1. Einstein SSS experimental spectra of two cataclysmic variables.

Figure 1 displays some raw data from the Einstein SSS from two of these systems. The effective temperature of the $\sim 10^8$ K continuum is not sensitively measured by this instrument, because its dynamic range is in the region of the spectrum where the continuum is quite flat. The temperatures chosen were determined from higher energy data from HEAO A-2 and, as can be observed from the solid traces representing the model inputs folded through the detector response as described in the lecture devoted to SNR spectra (Holt, this volume), the fit to the SS Cygni data is quite good. The EX Hydrae data, even though their statistical quality are poorer, cannot be fit by the high temperature component alone. Virtually all of the structure in the EX Hydrae spectrum can be reconciled with an additional component (at the $\sim$ 1% level) of lower temperature emission which is characterized by the strong resonance emission lines from He-like Si and S. SS Cyg and U Gem (in outburst) have exhibited intense components at even lower temperatures ($\lesssim$ 100 eV) which are pulsed on timescales of seconds.

Kylafis and Lamb (1979) have generalized the problem of accretion onto a white dwarf to carefully consider cases for which the accretion rate approaches the Eddington-limited conditions. They find a peculiar relation between the apparent X-ray temperature and the luminosity which is double-valued, and Copernicus data from Cyg X-2 are apparently in agreement with this relation (Branduardi 1977). Using these calculations, the measurement of the apparent temperature and flux at the Earth fixes the distance to the source and, hence, allows the determination of the absolute luminosity and even the mass. The only difficulty with the model is the identification of sources for which it might be applicable; in particular, recent data (Cowley, Crampton and Hutchings 1979) suggest that the proto-typical case for the analysis, Cyg X-2, is

almost certainly a neutron star. It is unfortunate that this, one of the few model calculations which allows the inference of detailed physical information about the source from its spectrum (i.e. mass and absolute luminosity), may not have any unambiguous candidates to which it can be applied.

3. BULGE SOURCES

The large fraction of galactic X-ray sources have no pronounced spectral features (e.g. emission lines or sharp spectral breaks). They can generally be fit with a bremsstrahlung continuum at a temperature of several keV; deep exposures from satellite experiments may require deviations from a single temperature continuum, but the required deviations are often non-unique. If we exclude supernova remnants, X-ray pulsars and cataclysmic variables, the great majority of the others fall into this spectroscopic category.

Without additional information, such as we might obtain from the determination of binary periods, for example, we have no real handles on the nature of the compact objects or the binary system masses or separations. Sco X-1 and Cyg X-2, for example, which have always been characterized as similar based upon X-ray spectra and variability, have turned out to be in binary systems with very different periods: less than one day, and more than one week, respectively. Many of the others may be associated with the low mass ultra-short period systems recently suggested by Joss and Rappaport (1979). The remainder of this section will be devoted to the phenomenological description of the typical spectral characteristics of all the sources which are not known to be SNR, cataclysmics or X-ray pulsars, which include "soft" transients and bursters as well as "steady" X-ray sources. As their similarities far outweigh their differences, it is likely that most of them have a common origin in a neutron star accreting mass from a binary companion.

After the approximately thermal nature of the overall emission, the next most striking similarity in the X-ray emission is the considerable variability in intensity. Even before the consideration of "burst" or "transient" emission episodes, in which the emission level may change by orders of magnitude, almost all of the sources are variable by at least a factor of two or so on timescales of days or more. Furthermore, this variability seems to be correlated, on the average, with luminosity. This was first detected by the UCL group for Sco X-1 (White et al. 1976) but it appears to be generally (or at least typically) true. In Figure 2 the ratio of "hard" to "soft" X-rays are plotted for two variable sources, and there is a clear correlation between spectral hardness and intensity level, i.e. the sources appear "hotter" when they are more luminous. It is worth noting, however, that Cyg X-2 has, on at least one occasion, exhibited a departure from this monotonic behavior, as mentioned in Section 2.

The detection of unambiguous Fe-K features from diffuse X-ray sources and X-ray pulsars has led to the search for such features in the other sources, with quasi-negative results. The "quasi" is an important qualification, because while all searches for narrow line

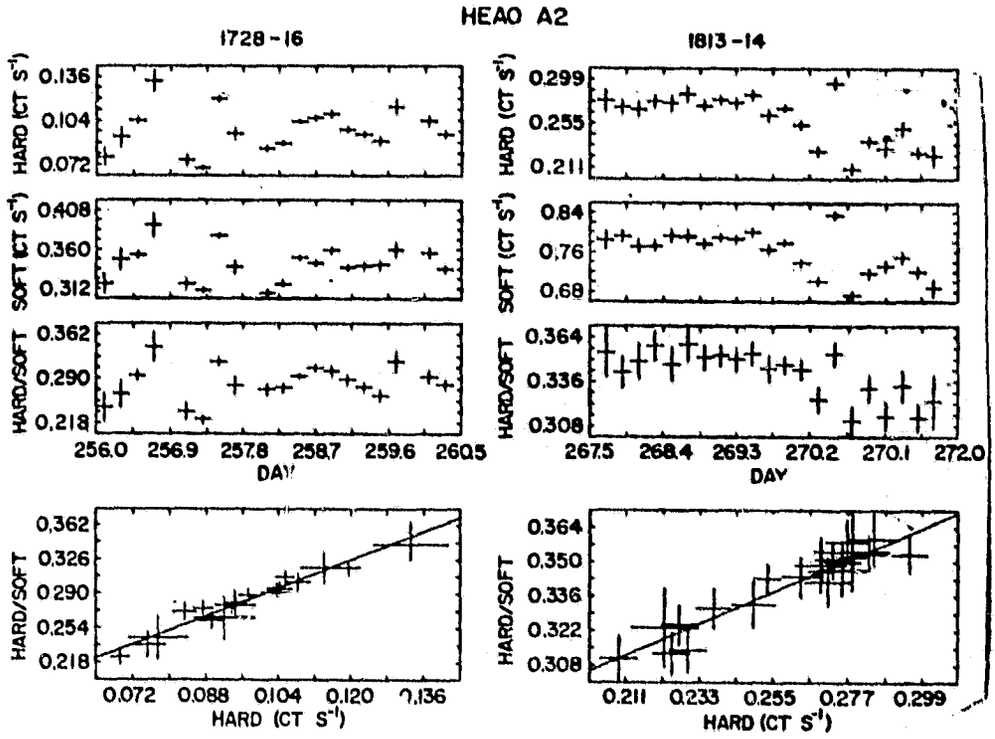

Fig. 2. HEAO A-2 "hardness ratios" for two bulge sources, indicating the correlation between spectral hardness and intensity.

features have been unsuccessful (some with upper limits to the line equivalent widths as low as ∿ 2 eV), there are persistent indications of very broad Fe features with equivalent widths in excess of a few hundred eV. The nature of these indications are reductions the χ^2 in the fitting procedures (rather than actually discernable features), but such broadened line emission might well be expected from objects which are observed through a large Thomson optical depth. Typically, the overall spectra can be consistently reconciled with this assumption.

The last spectral feature worthy of note in this section is the signature of Type I bursts. The Type II bursts of the "rapid burster" are not spectrally distinct from the average properties of the sources discussed here, nor do they appear to exhibit any spectral evolution within a burst. Type I bursts, on the other hand, have a pronounced black body character which differs considerably from the average source behavior. Furthermore, this spectrum appears to cool just like a black body throughout the burst (i.e. the radius of the burst region remains constant, at a value consistent with that of a neutron star). This spectral pecularity, first noted by Swank et al. (1977), has been used by van Paradijs et al. (1979) to argue that the burst sources are neutron stars, as the Type I bursts are consistent in all respects with He-burning episodes on neutron stars as calculated by Joss (1979).

There are some "anomalous" sources which do not fit neatly into the two broad categories I have defined: the "pulsars" discussed in

the next section, and the "bulge sources" described here. The prime black hole candidate Cyg X-1, for example, exhibits a power law spectrum which is remarkably constant in both slope and intensity with time in the range 1-100 keV, at least during the extended "low" states which constitute the large fraction of the source history. Even though Cyg X-1 exhibits considerable microstructure on timescales < 1 sec, on timescales > 1 hour it is one of the most stable sources in the galactic catalog. This must clearly represent a true steady-state condition, and Sunyaev and Trumper (1979) have recently modelled the emission as arising from the superposition of Thomson-scattered components of an accretion disk around a black hole. In marked contrast, the second black hole candidate Cir X-1 is erratic on any timescale. Its spectrum often appears to be similar to that of the bulge sources, but the absorption at low energies is considerably more variable than most, and there is clear evidence for Fe-K emission which is more than merely inferential. The similarity between the two black hole candidates in temporal microstructure does not extend to the X-ray spectrum; this may not be a strong yes-no discriminator for the presence of a black hole, however, as the spectrum is likely to be dominated by the geometry far from the central mass.

No discussion of spectra of galactic X-ray sources can be complete without at least a mention of Cyg X-3. Like Cyg X-1, its spectrum can be generically characterized as bimodal with a "high state" which can be roughly fit with a black body at a few keV and a "low state" which can be better fit by a much flatter power law which extends to higher energies (interestingly, the total X-ray luminosity in both cases is the same close-to-Eddington-limited luminosity for a unit solar mass). The prime characteristics of this source are an enormous column density (virtually no emission below $\sim$ 1.2 keV can be detected through such a column), and the most pronounced Fe-K emission line yet observed (Serlemitsos et al. 1975). The Fe line alone would easily rank among the 50 brightest (in apparent X-ray magnitude) sources in the sky. This line arises from fluorescence of the material responsible for the large column density around the hot source embedded in the cloud, and the SSS has recently detected S fluorescence, as well. There is a reproducable asymmetric temporal modulation of 4.8 hours ascribed to the system binary period, and with all these temporal and spectral clues we still cannot unambiguously pin down the source geometry (i.e. whether the thick material is a stationary shell or a wind from the companion) or even the nature of the compact object.

4. X-RAY PULSARS

Those sources which have periodic modulation of their X-ray emission on timescales $\lesssim$ 1000s have been termed "X-ray pulsars", even though they are quite different physical systems than the Crab nebula. The Crab pulsar is the only true X-ray "pulsar", as it is losing rotational kinetic energy with time. All of the dozen or so others (which are the ones I shall discuss here), are magnetized neutron stars which are increasing their rotational kinetic energies, because they are accreting material with angular momentum in the same sense as that in which they are rotating.

Unlike the sources discussed in section 3, the X-ray pulsars have several spectral characteristics in common which are not shared by the bulk of the galactic X-ray catalog.

Perhaps the most obvious of these is the very hard ($0 \lesssim \alpha \lesssim 0.5$) energy index of the phase-averaged power-law spectrum. A second characteristic is the sharp cutoff of this spectrum above $\sim$ 20 keV. Only X Persei, which is less luminous by at least two orders of magnitude than the others, does not appear to exhibit such an extreme spectral shape. It should be noted here, as well, that fully half the sample of X-ray pulsars are associated with "hard" or "recurrent" transient sources, where the pronounced emission episodes are believed to arise from episodes of enhanced accretion onto the neutron stars.

Other spectral characteristics of the X-ray pulsars are variable low energy absorption, marked spectral variations throughout the pulse cycle, unambiguous Fe emission, and the possibility of cyclotron emission or absorption in at least two (and possibly all) of the sources. All of these spectral characteristics are interrelated, in the sense that they can be "explained" with a number of assumptions which is smaller than the number of spectral characteristics noted.

If we assume that the X-ray emission from these sources originates close to the neutron star from material which is funnelled into the polar regions by the magnetic field, all of the characteristics of the X-radiation may further be assumed to arise from geometrical considerations, i.e. "beaming" of some sort in the production process itself, and/or transport of the X-radiation through the infalling material. Basko and McCray and their coworkers have devoted considerable effort to the details of a model which has had some success in achieving consistency with the data from Her X-1, which is based on the presence of a semi-opaque shell of material at the Alven surface. This shell may allow an almost unobscured view of the source region for part of the pulse cycle, and is responsible (via Thomson scattering) for the reprocessing of X-radiation from the beamed radiation which intercepts the more opaque portions of the shell. The Fe-K emission is fluorescence from the shell. Pravdo and his coworkers have been responsible for most of the detailed spectral results from OSO-8 and HEAO A-2 with which the model has been refined.

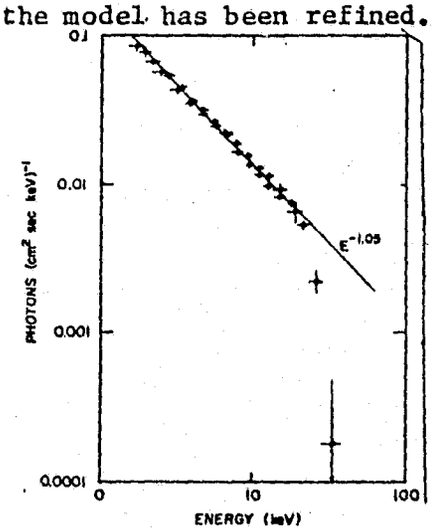

Fig. 3. Her X-1 spectrum obtained in a rocket flight.

Figure 3 is an early Her X-1 spectrum obtained from a rocket flight which has been "inverted" in accordance with equation 1.5 of the lecture on SNR spectra in this volume. The two types of points displayed represent data from two different proportional counter systems. Clearly evident from the figure is the hard power-law spectrum and sharp cutoff at higher energies. Less evident is the case for substantial Fe-K emission near 6.5 keV, although the points from both detectors are systematically above the best fit near that energy (and, it should be noted, the spectral inversion technique depresses such features if they are not assumed to be present in the input spectrum). Figure 4, taken from the OSO-8 satellite, should dispel any doubt that a substantial Fe-K feature is present in the Her X-1 spectrum. Both of the spectra displayed are raw counts, and the Fe-K feature is quite statistically significant in the left-hand spectrum, even though it does not appear obvious to the eye. The right-hand spectrum was obtained during an "absorption dip", and the fact that the Fe emission is absorbed less than its surrounding continuum makes the feature quite obvious. Such fluorescent Fe-K emission, with equivalent widths $\gtrsim$ 200 eV, are typical of X-ray pulsar spectra. For Her X-1, this equivalent width implies that the assumed opaque fraction of the obscuring shell is at least 0.5 (Pravdo 1978).

The study of spectra at differing pulse phase can sometimes offer unique insight into the system. The most elementary form of "pulse-phase-spectroscopy" is the display of the pulse profile in different energy bands. The first attempt at this sort of display was from the rocket data shown in Figure 3; this is shown in Figure 5, where the residuals of the pulse shape at differing energy bands compared to the

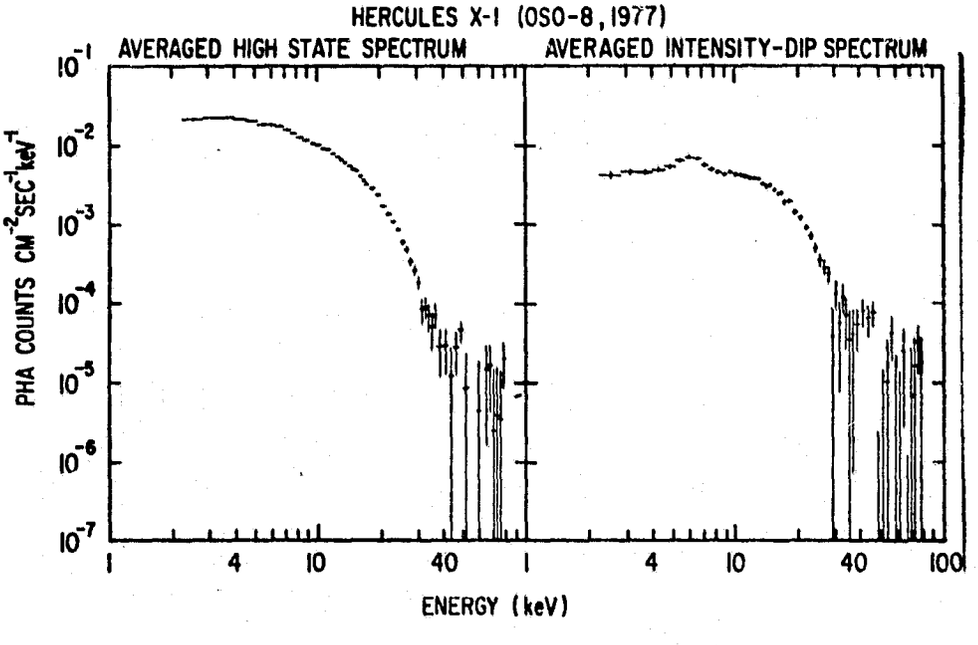

Fig. 4. OSO-8 experimental spectrum of Her X-1.

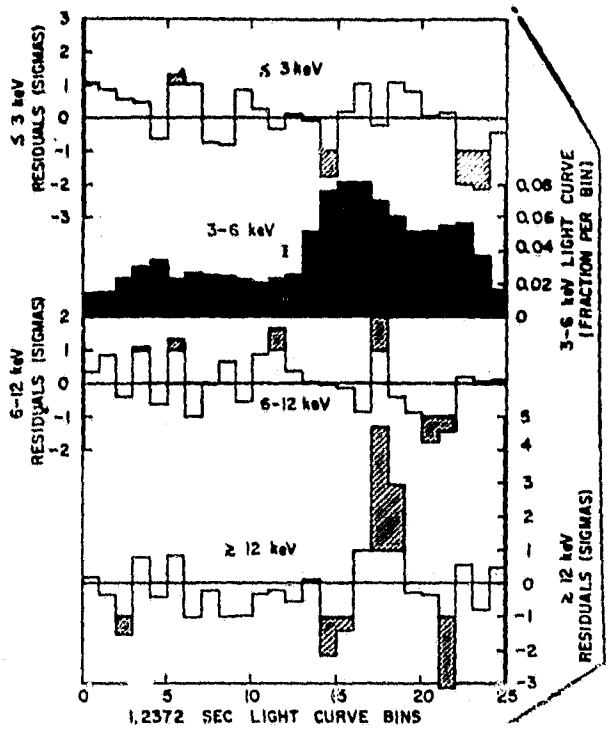

Fig. 5. Her X-1 data of Fig. 3 sorted into 25 pulse phase bins and 4 energy bins. Using the 3-6 keV light curve as a template, the residuals of the other three light curves are plotted (those > 1σ are shaded for emphasis).

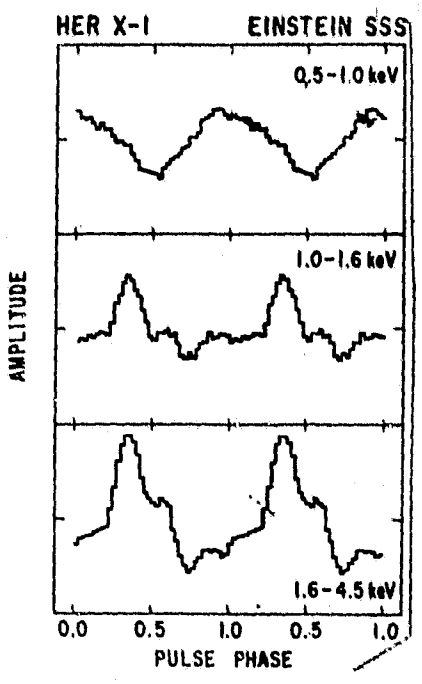

Fig. 6. Einstein SSS data from Her X-1 in three energy ranges as a function of pulse phase.

3-6 keV template are displayed. The only clear indication of energy dependence in this very early analysis was the indication of hardening during the falling portion of the main pulse. Confirmation of this effect was found in OSO-8 data, and Pravdo et al. (1977) suggested that this hardest portion of the spectrum represented the most unobscured view we could obtain of the primarily produced spectrum, with the bulk of the pulse phase dominated by the softer radiation reprocessed at the Alven shell. New data from Einstein seems to confirm this supposition (see Figure 6), as the radiation below 1 keV has its minimum in phase with the hardest spectrum at higher energies.

The sharp cutoff at ∿ 20 keV is almost certainly related to the high magnetic field at the neutron stellar surface, either through its effect on Compton scattering or via cyclotron absorption. In addition, J. Trumper and his associates have detected the presence of emission near 50 keV and have interpreted its origin in terms of cyclotron emission. There is now no doubt that the source is detectable at 50 keV and undetectable at slightly lower energies (see Figure 4), although there may still be some controversy regarding the interpretation of these data. At least one other source, the transient 0115+63, may exhibit spectral features which have been interpreted in terms of a cyclotron

origin. It should be emphasized, however, that the interpretation of features which are phase-dependent (as is the case with the 0115+63 feature) is non-unique, as there is no unambiguous way to determine the correct "unpulsed" contribution to subtract from the measurement.

5. STARS

The advent of the HEAO-1 satellite resulted in the discovery of X-ray emission from a large number of late-type RS CVn stars, and HEAO-2 is increasing the sample to include earlier (and later) stars, as well. The SSS has studied several of the late-type systems, and has measured thermal emission features from many of them. The only analysis which is mature at this time is that of the nearby Capella system, but it probably is exemplary of what the RS CVn spectra will yield.

The data cannot be fitted with a single temperature (even with the abundances variable), but can be fitted with two temperatures with variable abundances. The single temperature best fit is at a temperature of $\sim 8 \times 10^6$ K with abundances which are near-solar, while the two-temperature fit (at $\sim 6 \times 10^6$ K and $\sim 40 \times 10^6$ K) requires abundances which are approximately 3 times solar. The data can also be fitted with a distribution of temperature components which has a peak just below 10^7 K, but which extends from $\sim 5 \times 10^6$ K to $\sim 5 \times 10^7$ K. Figure 7 displays the data fitted with the best-fit two-temperature model described above, the same less Fe, and the two temperature components separately. Clearly, the emission lines of Fe(L), Mg(K), Si(K) and S(K) are constraining any fits to the spectrum to peak just below 10^7 K and to require some emission up to at least 3×10^7 K.

Most coronal models derive the heat input to the corona from acoustic pressure from the photosphere which is converted in the transition region to heat the gas. This process is usually sorely pressed to heat the corona to temperatures much in excess of 10^6 K, so that the Capella measurement described here requires some rethinking of the heat input to such stars. Rosner, Tucker and Vaiana (1978) have suggested that the coronae of late-type stars may be composed of magnetic loop structures in which the hot plasma is contained; in such a scenario, the heating is accomplished via the conversion of magnetic energy. RS CVn stars, in particular, are more starspot-active than is the Sun, but even the solar corona appears to be composed of such loop structures.

In a loop model, the temperature of the X-ray emitting plasma depends only on the pressure (and, hence, the magnetic field) and the size of the loop, so that we would expect a peak in the emission measure distribution characteristic of the "typical" loop, but we should not be surprised to find a high temperature tail to this distribution arising from atypical structures on the stellar surface. The spectrum observed was constant over several hours, so that these loops constitute a stable configuration. Since the X-ray emitting gas is much too not to be gravitationally bound to the star, the magnetic confinement in the loops prevents catastropic mass loss from the corona. It is interesting to note that Ayres and Linsky (1979) have recently concluded from independent evidence obtained with the IUE satellite that the G0 secondary of the Capella system is very similar to the starspot-active component of RS CVn systems.

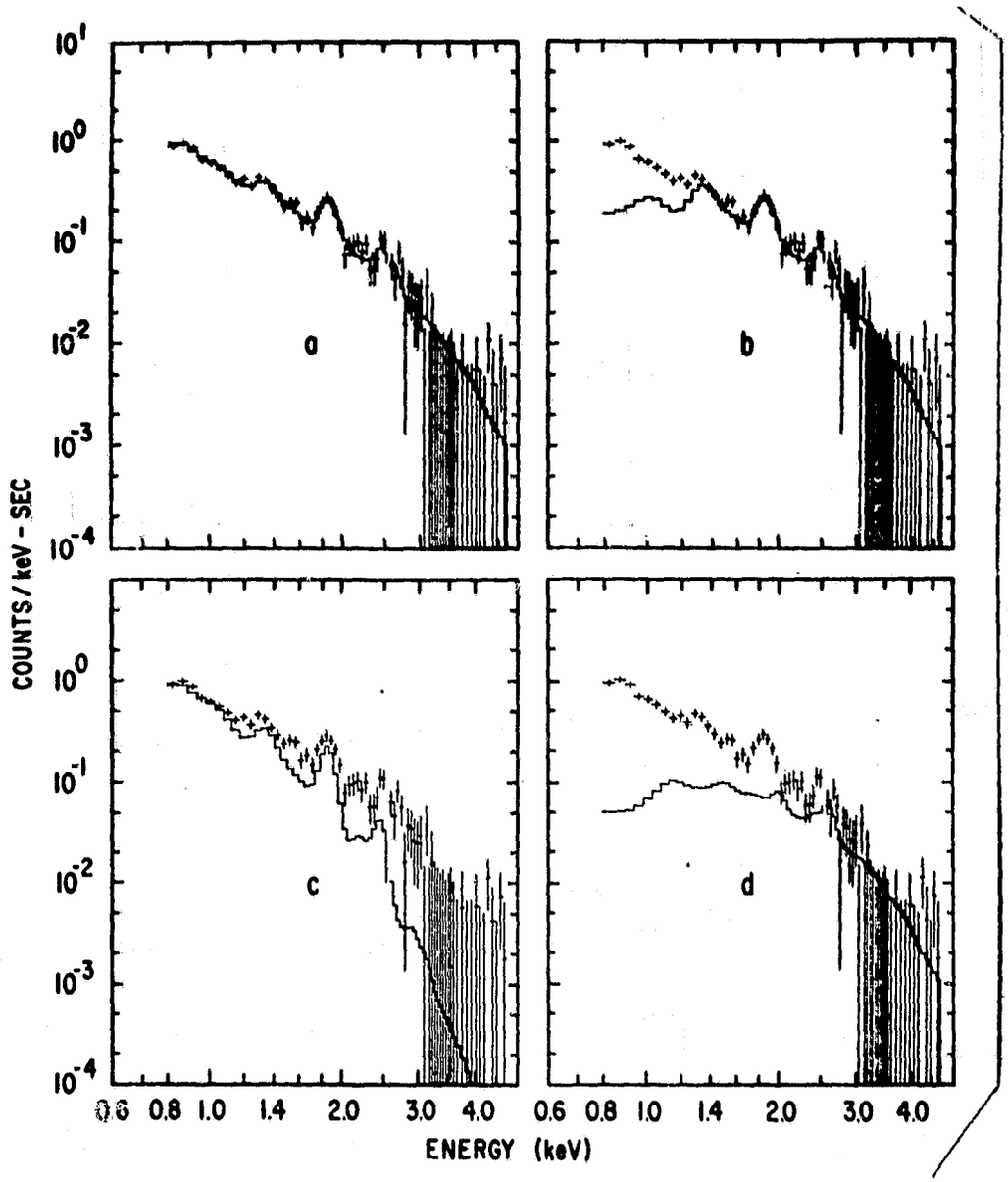

Fig. 7. Einstein SSS data from Capella fitted with a two-component collisional equilibrium model (a), the same with Fe abundance set equal to zero (b), and the lower temperature (c) and higher temperature (d) components alone.

REFERENCES

Ayres, T.R. and Linsky, J.L., 1979, B.A.A.S. 11, 472.
Branduandi, G., 1977, Ph.D. Thesis, Univ. of London.
Cowley, A.P., Crampton, D., and Hutchings, J.B., 1979, Ap. J. 231, 539.
Fabian, A.C., Pringle, J.E., and Rees, M.J., 1976, M.N.R.A.S. 175, 43.
Joss, P.C., 1978, Ap. J. (Letters) 225, L123.
Joss, P.C. and Rappaport, S., 1979, Astron. Ap. 71, 217.

Kylafis, N.D. and Lamb, D.Q., 1979, Ap. J. (Letters) 228, L105.
Pravdo, S.H., 1978, in Proc. XXI COSPAR/IAU Symposium in X-ray Astron. (Pergamon Press, Oxford).
Pravdo, S.H., Becker, R.H., Boldt, E.A., Holt, S.S., Serlemitsos, P.J. and Swank, J.H., 1977, Ap. J. (Letters) 215, L61.
Pringle, J.E. and Rees, M.J., 1972, Astron. and Ap. 21, 1.
Rosner, R., Tucker, W.H., and Vaiana, G.S., 1978, Ap. J. 220, 643.
Serlemitsos, P.J., Boldt, E.A., Holt, S.S., Rothschild, R.E., and Saba, J.L.R., 1978, Ap. J. (Letters) 201, L9.
Sunyaev, R.A. and Titarchuk, L.L., 1979, preprint.
Sunyaev, R.A. and Trumper, J., 1979, Nature, in press.
Swank, J.H., Becker, R.H., Boldt, E.A., Holt, S.S., Pravdo, S.H., and Serlemitsos, P.J., 1977, Ap. J. (Letters) 212, L73.
van Paradijs, J., Joss, P.C., Cominsky, L. and Lewin, W.H.G., 1979, Nature, in press.
White, N.E., Mason, K.O., Sanford, P.W., Ilovaisky, S.A., and Chavalier, C., 1976, MNRAS 176, 91.

X-RAY SPECTRA OF ACTIVE GALACTIC NUCLEI

S.S. Holt

Laboratory for High Energy Astrophysics
NASA/Goddard Space Flight Center
Greenbelt, Maryland 20771 U.S.A.

1.0 ACTIVE GALACTIC NUCLEI

There are a variety of galaxies which are classified as nuclear-active, ranging from those which have nuclei which are merely distinguishable from a stellar component all the way to QSO's. The subject of this lecture will be only those extreme cases (Seyfert I, BL Lac and quasar) which constitute the most intense compact X-ray sources which are presently known. The luminosities of these sources in the 2-10 keV band range upward of 10^{42} ergs/s (to more than 10^{46} ergs/s), while those sources classified Seyfert II or NELG are typically less luminous.

The main distinguishing characteristic of these objects is not their absolute luminosity, but the extent to which the nucleus is a compact luminous entity. The prime defining characteristic of Sy I nuclei is the very broad ($\gtrsim 10^4$ km/s FWZI) emission lines which emanate from the central portion of the nucleus, upon which the much narrower ($< 10^3$ km/s) lines from the surrounding region are superposed: Sy II spectra contain only the "narrow" lines, while Sy I contain both. The central broad-line-region (BLR) is generally taken to have a characteristic dimension $\lesssim .05$ pc, based upon the timescale for variability observed, and the surrounding NLR may have a characteristic dimension of ~ 1 kpc. Forbidden lines are only observed from the NLR, so that the electron density in the BLR optical filaments must be $\gtrsim 10^8$ cm^{-3}. The X-ray emission appears to correlate with continuum and line emission from the BLR, so that we expect that this central region of these nuclei is the site of the X-ray emission; indeed, the shortest timescale for variability from at least one of them, NGC4151, is less than one day. A recent review of the properties of X-ray emitting Seyfert galaxies and their correlations with emission in other bands may be found in Wilson (1979).

The current prevailing opinions place the energy source for the luminosity of these objects in a central black hole (or equivalent) of mass $\sim 10^8$ $M_\odot$. Quasars are assumed to be the most extreme cases of Sy I, and BL Lac nuclei are also assumed to be closely related (the latter objects differ from Sy I in four

respects: they are generally in elliptical rather than spiral galaxies, they are strong variable radio emitters, the optical emission lines are very weak or undetectable, and their optical emission is highly polarized).

The X-ray emission from these nuclei, as in the case of binary X-ray sources, cannot be assumed to emerge without substantial Compton scattering. Fabian (1979) has recently reviewed the possible mechanisms which might be most directly responsible for the X-rays observed. If there exists very hot plasma ($T \gtrsim 10^{8}{}^{o}K$), as might be expected from shock heating or accretion onto the central object, there will be a direct bremsstrahlung component which will emanate from the nucleus. The presence of the non-thermal continuum in the BLR will favor X-ray production via Compton scattering from the high temperature electrons, however, so that the spectrum may not be easily interpretable even if these were the only possibilities. The presence of ultrarelativistic electrons ($\gamma \gtrsim 100$) complicates the story further, as X-rays may be produced from Compton interactions of these electrons with the far infa-red synchrotron radiation which they produce in the ambient magnetic field. The primarily produced X-radiation may be further Compton-scattered before emerging from the source region, as well.

All of the X-ray measurements are obtained over limited dynamic ranges, so that the bulk of this lecture will be devoted to a review of the search for consistent characteristics of the spectra of active galactic nuclei which we might hope to ultimately reconcile with detailed models.

2.0 SEYFERT I SPECTRA

A sample of seven Seyfert I spectra obtained with HEAO A-2 in the energy range 2-50 keV have recently been analyzed by Mushotzky et al. (1979b). The spectra are generally better-fit by power-laws than by bremsstrahlung continua, so that a power-law representation will be utilized for all of them. Five of the seven "inverted" spectra are displayed in Figure 1.

If we consider the spectra > 5 keV, all can be fit to single power-law forms. Figure 2 illustrates the best-fit and range of acceptable indices for each of them, as a function of source luminosity. It appears from this sample that there is no obvious correlation of spectral index (the label α is used in the Figure for the photon spectral index, which is higher by unity than the index of the energy spectrum) with luminosity, and that the entire sample is consistent with an energy index of 0.6 - 0.7. The simple average of all the indices measured from this sample is 0.65, but the weighted average is closer to 0.6 since a high exposure to NGC4151 makes the formal statistical quality of that index better than the others. There is no evidence for steepening at the highest energies we measure in any of the spectra (although they must clearly steepen eventually).

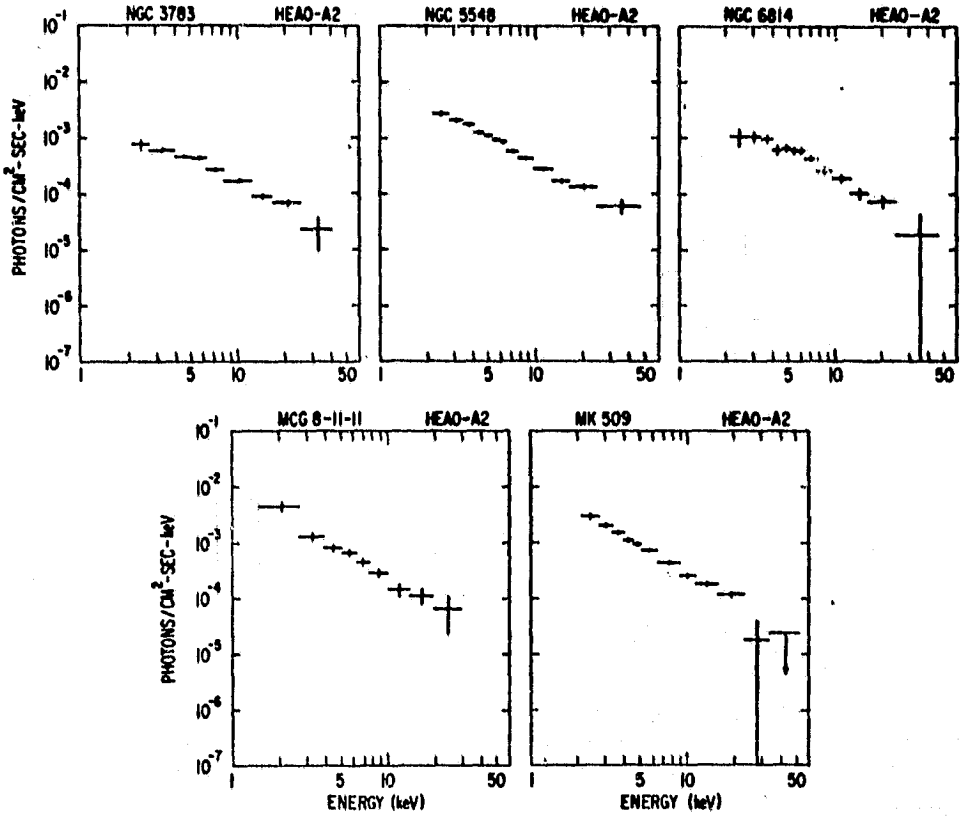

Fig. 1. Incident X-ray spectra of five Seyfert I galaxies.

There is clear evidence for variability in about half the sample (the HEAO-1 satellites measures each at six month intervals, so that all may be variable to some extent). The highest degree of variability has been measured from the least luminous sources (NGC3783 was measured to vary by more than a factor of two in less than one week, and NGC4151 by a like amount in less than one day). We cannot be sure that this apparent inverse correlation with luminosity is real because of the small sample, but there does not appear to be any change in spectral index for any of these sources with intensity.

Below 5 keV there are two effects which deserve consideration. The first is that substantial absorption attributable to nonionized material has been measured only from NGC4151; this absorption changes on short timescales and has been, therefore, attributed to the optical filaments within the BLR (Ives, Sanford and Penston 1976). The only other objects for which absorption corresponding to a column density in excess of $N_H \sim 10^{22}$ cm^{-2} has been inferred are NGC3783 and NGC6814, so that we have an indication that the lower luminosity Sy I sources are more likely to exhibit such an effect.

The other low energy characteristic of these objects is a

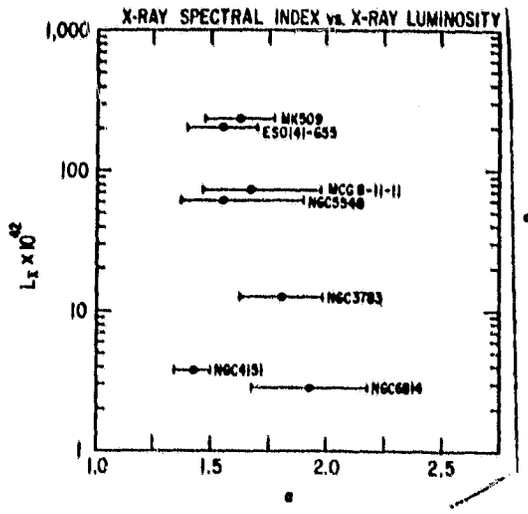

Fig. 2. Photon power-law index versus 2-10 keV X-ray luminosity for seven Seyfert I galaxies.

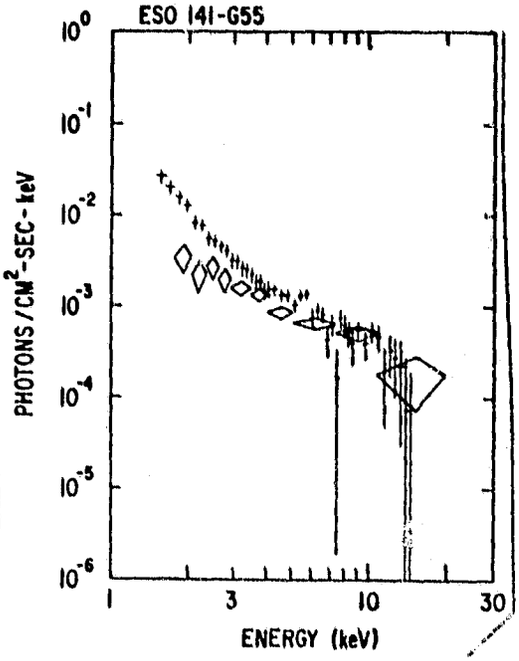

Fig. 3. Two separate HEAO A-2 measurements of the spectrum of ESO 141-G55.

variable excess below 5 keV that is exhibited by at least some of them. Figure 3 displays the spectra from two exposures of ESO141-G55, which illustrates the steepening below 5 keV in one (the crosses) while consistency with the other (the diamonds) above 5 keV is achieved. A single 0.8 - 4.5 keV measurement of ESO141-G55 with the Einstein SSS measured this steep component, as well.

The overall characteristics of this sample, therefore, indicate that NGC4151 is hardly prototypical. In fact, NGC4151 has an anomalously hard spectrum, and anomolously large low energy absorption (in both cases, representing the extreme for the sample). The other Seyferts may, in fact, exhibit excesses rather than deficiencies at low energies. All may be variable (no others have been detected to vary on timescales as short as NGC4151, but this may reflect a selection effect because NGC4151 has the highest apparent magnitude), and all appear to preserve their characteristic power law index above 5 keV if they do vary. The average index for the total sample is consistent with the statistical errors for each of the individual members of the class. Sy I objects analyzed after completion of the study from which Figures 1-3 are taken, NGC7469 and MCG-2-58-22, have HEAO A-2 and Einstein SSS spectra completely consistent with the sample characteristics discussed here.

3.0 BL LAC SPECTRA

The BL Lac sample at our disposal is less than half as large as that for Sy I, and the initial results led to what probably represented a premature characterization of their average spectra. Mushotzky et al. (1978) noted the hardness of the initial measurements of Mk421 and Mk501 ($\alpha \approx 0.2$), although there was some evidence for steepening at low energies in both of these objects. We later found (Mushotzky et al. 1979a) that Mk421 also exhibited variability in the soft component on occasion, and that the hard component could vary by at least a factor of 4 (see Figure 4).

On the basis of several exposures to MK421, Mk501, PK0548-322, 2155-304 and 1219+305 from both HEAO A-2 and the Einstein SSS, we now believe that all the BL Lac sources exhibit spectra which can be synthesized from two power-law forms: a very hard component ($\alpha \approx 0.2$) and a much softer ($\alpha \approx 2$) component. We have never measured any evidence for absorption ($N_H < 3 \times 10^{21}$), which may or may not be related to the absence of optical emission lines, and the hard component appears to be more highly variable than does the soft component. In other words, an arbitrary BL Lac spectral measurement is likely to yield evidence for a steep spectral component more than half the time (and more often than a hard component).

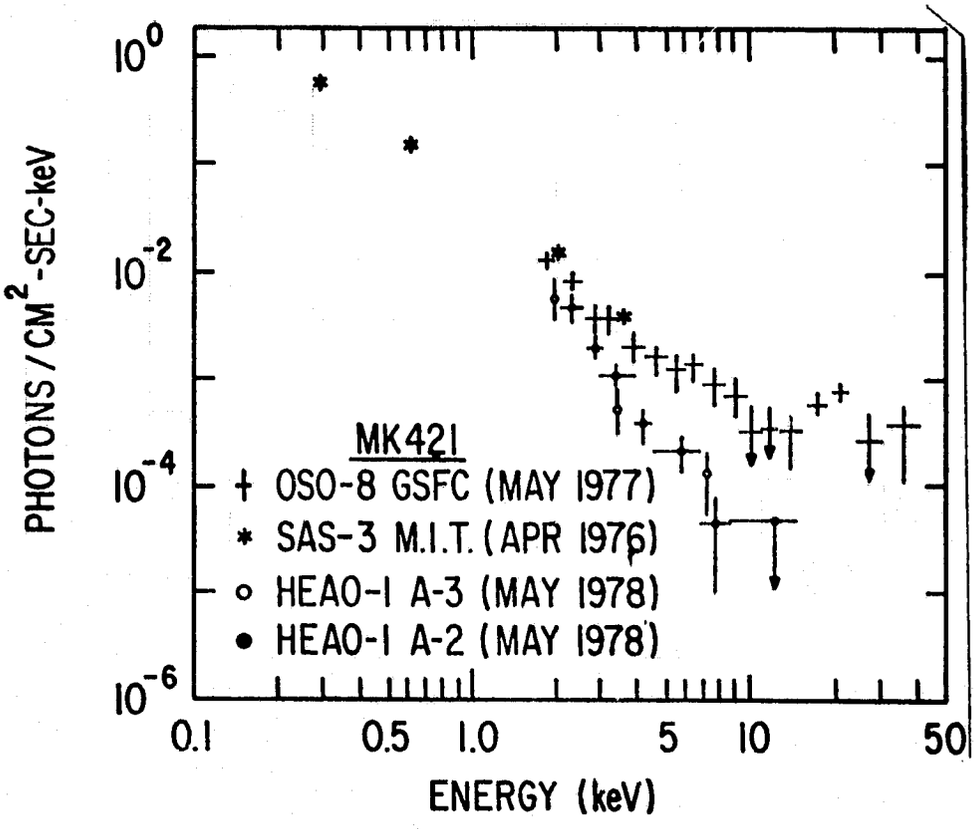

Fig. 4. Four separate measurements of Mk421.

4.0 QUASAR SPECTRA

The situation here is even more sparse than for BL Lac's. Several exposures have been made to 3C273, but we have no correspondingly deep exposures to any other quasars above a few keV except for 0241+62. The latter source is well-fit by a Crab-like spectrum out to 50 keV (i.e. steeper than the Sy I average index), and Fairall 9 is well-fit by a similar index below 4.5 keV with the Einstein SSS. More SSS spectra of quasars will be available in the near future, but only at energies commensurate with the 0.8 - 4.5 keV window of the SSS.

3C273 has been measured on several occasions by HEAO A-2. It has exhibited 40% variations on timescales of 6 months, and best-fit energy indices between 0.41 and 0.73 (the statistical errors in the latter include the former, but not vice versa). The deepest exposure measured the hardest overall spectrum out to $\sim$ 60 keV (the steepest was the observation which was 40% lower in intensity), but there was some marginal evidence for steepening with lower energy (as well as evidence from another instrument on-board HEAO-1 for steepening above 60 keV). A detailed description of the HEAO A-2 3C273 observations is given in Worrall et al. (1979), as well as appropriate references to the data at higher energies.

Based upon such a limited sample, one should be careful not to prematurely assume class properties of quasar spectra. In particular, the brightest quasar 3C273 may be just as spectrally anomalous as the brightest SNR (the Crab nebula) and the brightest Sy I (NGC4151) have turned out to be.

5.0 THE DIFFUSE BACKGROUND

Many researchers have independently deduced that a large fraction (perhaps all) of the presently unresolved "diffuse X-ray background" (XRB) may be composed of discrete sources. In particular, recent evidence would suggest that the main contributor is required to arise from a population of objects with a strong evolutionary character (e.g. Avni 1978). Several investigators (e.g. Setti and Woltjer 1979) have suggested that quasars might naturally provide the required evolutionary behavior. Schwartz (1978) has emphasized that spectral and luminosity constraints (via the observed limits on XRB spatial fluctuations) exist on candidate populations, and the remainder of this lecture will be devoted to one such constraint.

The issue I am addressing is to what extent the measured spectrum of the XRB is consistent with the spectra of candidate populations. I shall not consider the very important further constraints (e.g. fluctuations, volume emissivity functions, evolution) which are essential to the whole story because I do not want to confuse the effects of other assumptions with the very specific constraint imposed by the spectrum.

Marshall et al. (1979) have recently reported a systematic-

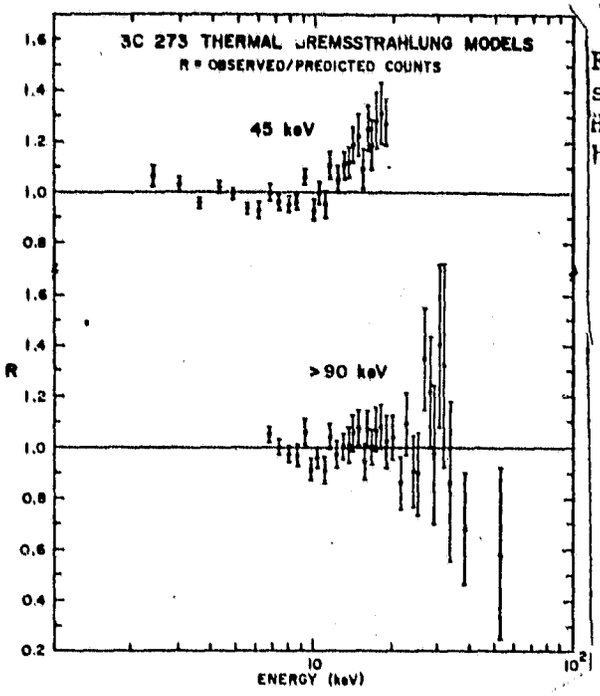

Fig. 5. Ratio of 3C273 spectrum measured from HEAO A-2 to expectation from bremsstrahlung continua.

free measurement of the XRB from HEAO A-2. Below $\sim$ 3 keV the galactic and extragalactic contributions cannot be unambiguously separated, and above $\sim$ 50 keV the experiment rapidly loses sensitivity. Between these two limits the spectrum is remarkably well-fit by thermal bremsstrahlung from a 40 $\pm$ 5 keV plasma. Field and Perrenod (1977) have discussed the possibility of a true intergalactic plasma which might give rise to this spectrum, and approximately 1/3 the closure density would be required to match its intensity without clumping (a non-homogeneous plasma would require a smaller density). The quality of the fit does not necessarily demand a thermal bremsstrahlung origin for the XRB, or even a substantial fraction of it. It does, however, define the spectral conditions which the totality of the XRB contributors must meet.

3C273 is the best-measured of the quasars, and a comparison of its spectrum with the XRB is encouraging, as evidenced by Figure 5. A direct comparison fails, as shown by the top trace, but if we assume that quasars like 3C273 must be at $Z > 1$ we can achieve consistency at least over a limited dynamic range, as demonstrated in the lower trace. The fit is acceptable over a dynamic range of about 4 (it fails below 6 keV (not shown), but that may not be too serious because there are other XRB contributors and possible galactic complications there), as compared to a dynamic range of 15 in the HEAO A-2 XRB spectrum. It meets the necessary condition for being a consistent contributor to the XRB, but not the sufficient condition. Unfortunately, it cannot be tested in the crucial region near 40 keV where it should rapidly steepen. The positive detection of 3C273 by Cos B at γ-ray energies may indicate that

it cannot steepen rapidly enough at reasonable redshift, and Setti and Woltjer (1979) have suggested, therefore, that 3C273-like quasars would have to comprise no more than 5% of those from which the XRB arises.

The other two quasars for which the Goddard group has spectra are 0241+62 and Fairall 9, which both have exhibited power-law spectra similar to that of the Crab nebula (the latter below 5 keV, and the former between 2 and 50 keV). The only other spectra we possess which may be relevant to the question are the Sy I and BL Lac spectra discussed earlier, since the physical conditions in their nuclei may be similar to those in quasars (there is no evidence that their volume density evolves in the same manner, but I prefer to restrict myself to spectral consistency only as discussed above). The Sy I spectra are all steeper than the XRB with the exception of NGC4151, and the γ-ray measurements of NGC4151 constitute an even stronger spectral constraint than in the case of 3C273 against objects identical to that one contributing substantially to the XRB. The only measured spectra which are flatter are the hard components of the BL Lac's which are occasionally measured along with the much steeper (and more frequently observed) components. We are left, therefore, with the difficulty that the measured spectra from those active galactic nuclei which we expect to be most prototypical of those which can make up the XRB are all steeper. See Figure 6, where the ratio of the measured XRB spectrum to assumed power laws of $\alpha = 0.4$ and $\alpha = 0.7$ are plotted, for an indication of how serious this potential difficulty is even before steeper components arising from other origins are subtracted. The same ratio of the measured spectrum to thermal bremsstrahlung at 40 ± 5 keV is unity to within a few percent over the whole range.

The new evidence which has seemingly given experimental verification to the idea that the XRB is largely composed of the contribution from evolved quasars is the detection of such objects with the imaging instruments onboard the Einstein Observatory. Extrapolations can be made which suggest that the XRB may be thusly explained, but the spectral difficulty remains. Confining my remarks to spectral considerations only, there are a few subtle points worth considering. The first concerns the effective energies at which these observations are made. Using the response functions of the IPC and the HRI (Giacconi et al. 1979), the median energy of detected photons is always less than 1 keV for incident spectra steeper than an extrapolation to these energies of the 40 keV bremsstrahlung spectrum. The HRI median energy is always about a factor of two lower than that of the IPC in its pre-launch gain mode, so that it is always below ½ keV, even for the flattest candidate spectra. For the steep low energy components of Sy I and BL Lacs, which may be representative of at least some of the quasars, the median energy measured with the IPC is well below ½ keV. I shall assume, therefore, that the median energy which characterizes the imaging results is no higher than ½ keV. This

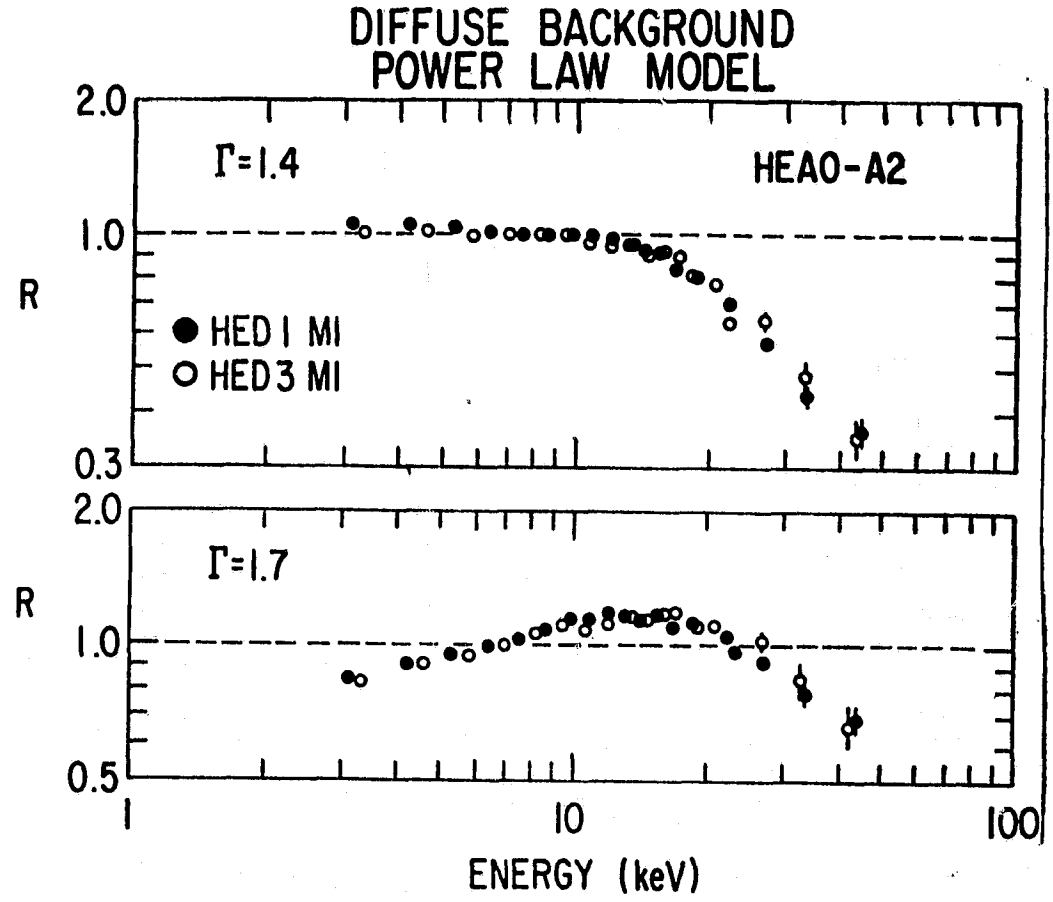

Fig. 6. Ratio of XRB spectrum measured from HEAO A-2 to expectation from power law continua.

means, therefore, that the imaging results are at an energy two orders of magnitude below the apparent thermal "peak" in the XRB, and two orders of magnitude above the peak in the optical cosmic spectrum which arises from starlight. We know that the starlight peak in the eV range has nothing to do with the X-ray background two orders of magnitude higher in energy, and the same orthogonality between the quasar images below 1 keV and the XRB at tens of keV may obtain if the quasar spectra are steep enough.

A quantitative estimate is clearly in order at this point, and Table 1 summarizes such an attempt. The entries in the table are based on the following assumptions. I begin by assuming that a thermal bremsstrahlung spectrum characteristic of a 40 keV plasma is an adequate representation of the XRB everywhere (i.e. even below 3 keV and above 50 keV, where there is experimental evidence with which this assumption is inconsistent). I then subtract from this spectrum components which I am sure must contribute, although there is some uncertainty in the magnitude of this contribution;

TABLE 1

SYNTHESES OF THE X-RAY BACKGROUND SPECTRUM

MODEL	DESCRIPTION (SEE TEXT)	RATIO OF MODEL TO 40 keV THERMAL, NORMALIZED AT 5 keV, AT ENERGIES (keV): .1	.2	.3	.5	1	2	3	5	10	20	30	50	100
1	40 keV thermal T(40)	1.00	1.00	1.00	1.00	1.00	1.00	1.00	1.00	1.00	1.00	1.00	1.00	1.00
2	0.6 index power law P(.6)	.88	.89	.89	.89	.90	.93	.95	1.00	1.13	1.46	1.87	3.08	10.75
3	0.7 index power law P(.7)	2.86	2.33	2.07	1.78	1.47	1.22	1.11	1.00	.92	.86	1.09	1.54	4.30
4	$T(40) + 0.1\left\{P(.6) + T(5)\right\}$	.84	.86	.88	.89	.92	.95	.97	1.00	1.03	1.04	1.03	.97	.61
5	$T(40) + 0.1\left\{P(.6) + T(5) + P(1)\right\}$	.81	.83	.86	.76	.88	.92	.96	1.00	1.05	1.06	1.06	.98	.65
6	$T(40) + 0.1\left\{P(.6) + T(5) + P(3)\right\}$	----	----	----	.71	.81	.93	.97	1.00	1.04	1.06	1.03	.97	.61
MODEL	FRACTION OF "TOTAL" FROM:													
4	P(.6): unevolved Seyferts	.16	.12	.11	.10	.09	.09	.08	.08	.08	.09	.11	.15	.35
	T(5) : clusters	.10	.10	.10	.10	.09	.08	.07	.05	.02	----	----	----	----
	T(40): diffuse thermal	.76	.78	.79	.80	.81	.83	.85	.87	.90	.90	.89	.85	.65
5	P(.6): unevolved Seyferts	.10	.10	.10	.10	.09	.08	.08	.08	.08	.09	.11	.15	.34
	T(5) : clusters	.08	.09	.09	.09	.08	.08	.07	.06	.02	----	----	----	----
	P(1) : "flat" quasars	.26	.19	.16	.12	.09	.06	.05	.04	.03	.03	.03	.03	.09
	T(40): diffuse thermal	.56	.62	.65	.69	.73	.77	.80	.83	.86	.87	.86	.81	.60
6	P(.6): unevolved Seyferts	----	.02	.04	.07	.09	.08	.08	.08	.08	.09	.11	.15	.35
	T(5) : clusters	----	.02	.03	.06	.09	.08	.07	.06	.02	----	----	----	----
	P(3) : "steep" quasars	.97	.85	.67	.35	.09	.02	.01	----	----	----	----	----	----
	T(40): diffuse thermal	.02	.12	.26	.51	.74	.82	.84	.87	.53	.90	.89	.85	.65

I arbitrarily assume, for computational ease, that clusters with an average temperature of 5 keV and unevolved Seyferts with an average energy index of 0.6 each contribute 10% of the total at 1 keV. After subtracting these "contaminants", I compare the shape of the resultant difference with exactly the same 40 keV spectrum with which I began by normalizing the two at 5 keV. Since the fit is good in the "testable" region 3-50 keV (in fact, it is a better fit than is a power law of index 0.4 over the range 3-10 keV only), I reconstruct a synthesized XRB spectrum as the sum of a 40 keV thermal bremsstrahlung spectrum normalized to the same fraction of the original total 40 keV spectrum at 5 keV, plus the same cluster and Seyfert contributions, and compute the contributions of each component of the new total as a function of energy. No attempts are made at best temperature or fractional contribution fitting; I am interested here only in determining crude consistency or inconsistency.

I next go through exactly the same procedure, this time including a 10%-at-1 keV contribution from quasars with relatively flat Crab-like ($\alpha = 1.0$) or relatively steep ($\alpha = 3.0$) spectra in addition to the 20% already assigned to clusters and Seyferts. A compilation of the extent to which the unassigned fraction of the original 40 keV thermal bremsstrahlung spectrum is still consistent with a spectrum of the same shape is given in the top portion of Table 1 for each of the trials discussed. The bottom portion of the table indicates the fraction of the synthesized XRB spectrum which can then be ascribable to each presumed component. The important results are that the large fraction of the 3-50 keV XRB can still be consistently reconciled with a diffuse thermal

component for the trials I have chosen, even though the XRB below 1 keV may be dominated by the quasars if their spectra are steep enough. It is important to note that the synthesized XRB spectra all exceed the extrapolation of the 40 keV bremsstrahlung spectrum below 3 keV (which may or may not be true), as well as > 50 keV (which definitely is true; the unevolved Sy I contribution I have assumed would dominate the measured XRB above 100 keV).

The arguments in this section have not been aimed at demonstrating the necessity (or even consistency) of the XRB with a substantial diffuse thermal component. In fact, I began by attempting to satisfy the hypothesis that it could arise from discrete evolved components. The apparent inconsistency between the spectra of active galactic nuclei which have already been measured and the XRB may be leading me astray if the evolution extends to spectra as well as number density; if so, however, it only makes the difficulty of inferring the > 10 keV contribution from < 1 keV measurements even more acute. Such spectral evolution (in particular, quasars at $Z > 1$ with spectra characteristic of bremsstrahlung at $\gtrsim$ 100 keV) can remove the requirement of a substantial diffuse component, but there are no data of which I am aware (or no measurements which can be made with Einstein that I can imagine) which can unambiguously resolve the problem.

REFERENCES

Avni, Y., 1978, Astron. Ap. 63, L13.
Fabian, A.C., 1979, Proc. Royal Soc., in press.
Field, G. and Perrenod, S., 1977, Ap. J. 215, 717.
Giacconi, R. et al., 1979, Ap. J. 230, 540.
Ives, J.C., Sanford, P.W., and Penston, M.V., 1976, Ap. J. (Letters) 207, L159.
Marshall, F.E., Boldt, E.A., Holt, S.S., Miller, R., Mushotzky, R.F., Rose, L.A., Rothschild, R.E. and Serlemitsos, P.J., 1979, Ap. J. in press.
Mushotzky, R.F., Boldt, E.A., Holt, S.S., Pravdo, S.H., Serlemitsos, P.J., Swank, J.H. and Rothschild, R.E., 1978, Ap. J. (Letters) 226, L65.
Mushotzky, R.F., Boldt, E.A., Holt, S.S. and Serlemitsos, P.J., 1979a, Ap. J. (Letters), in press.
Mushotzky, R.F., Boldt, E.A., Holt, S.S., Marshall, F.E. and Serlemitsos, P.J., 1979b, Ap. J., in press.
Schwartz, D.A., 1978, Proc. IAU/COSPAR Symp. X-ray Astron. (Pergamon Press, Oxford).
Setti, G. and Woltjer, L., 1979, Astron. Ap. 76, L1.
Wilson, A.S., 1979, Proc. Royal Soc., in press.
Worrall, D.M., Mushotzky, R.F., Boldt, E.A., Holt, S.S., and Serlemitsos, P.J., 1979, Ap. J. (Letters), in press.

THE X-RAY SPECTRA OF CLUSTERS OF GALAXIES

Richard Mushotzky

Laboratory for High Energy Astrophysics
NASA/Goddard Space Flight Center
Greenbelt, Maryland 20771 U.S.A.

1. INTRODUCTION

Clusters of galaxies were established as a class of X-ray sources by observers on the Uhuru satellite (Gursky et al. 1971). These early results indicated that clusters were a powerful (L_X in the 2-6 keV band > 10^{44} erg/sec) and numerous ($\gtrsim$ 9) class of extragalactic X-ray sources. These early results also indicated that the sources were extended (Kellogg 1972; Kellogg and Murray 1974) with a characteristic size $\gtrsim$ .25 Mpc. Early spectral data (Kellogg, Baldwin and Koch 1974; Catura et al. 1972; Gorenstein et al. 1973) showed that the spectra were not strongly cutoff at low energies and could be fit equally well by power laws of energy index $\sim$ 1 or by the emission from optically thin hot gas (henceforth referred to as thermal bremsstrahlung and abbreviated as T-B) with a temperature of $\sim 10^{8}$°K.

These early results suggested several models for the origin of the X-ray emission. Among these were (1) the integrated emission from single galaxies (2) thermal bremsstrahlung from a hot intergalactic gas (3) inverse Compton scattering off the 3°K background. Models (2) and (3) provide definite spectral predictions. The inverse Compton model predicted power law X-ray spectra with no features while the T-B model predicted a thermal X-ray spectrum with no features since it was expected that the gas was primordial and had no heavy elements in it.

2. PRE-HEAO OBSERVATIONAL RESULTS

The most important result of the first generation X-ray spectrometers flown on OSO-8 and Ariel-5 was the detection of Fe emission from the Virgo, Perseus and Coma clusters of galaxies (Mitchell et

al. 1976; Serlemitsos et al. 1978). This feature was interpreted as emission from iron in collisional equilibrium with a hot gas. Thus it was dramatic proof of the T-B origin of the X-ray emission and demonstrated that the intergalactic medium in clusters was not primordial but, since it had Fe in it, had been processed through stars.

Further observations with OSO-8 (Mushotzky et al. 1978) and Ariel-5 (Culhane 1979) detected Fe lines in 5 more clusters and groups of galaxies (3C129, NGC1129 group, SC0626-52 and Centaurus) established that the Fe line feature was a common property of clusters and indicated that the Fe abundance in the intercluster gas was roughly constant from cluster to cluster at Fe/H $\sim$ 1.5 x 10^{-5} (approximately half solar). These observations implied that clusters and their member galaxies have undergone substantial evolution (DeYoung 1978) with material being ejected from stars into the intergalactic medium and mixing with primordial material.

In addition to the Fe emission line results the large number of spectra observed with reasonable statistics by OSO-8 and Ariel-5 (Mushotzky et al. 1978; Mitchell et al. 1979) showed that the shape of the continuum emission favored a T-B model. These results also showed that clusters possessed a range of temperatures from 2-10^{7o}K to 1.2 x 10^{8o}K. The temperature results enable one to calculate the emission integral, $\langle n_e^2 \rangle$ V, and bolometric luminosities of the clusters. These results indicate that the hot gas has $\sim$ 10% of the viral mass of the cluster and a density of $\sim 10^{-3}$ cm^{-3}. Thus the prime observational quantities determined for clusters were their iron abundance, temperature, emission integral and bolometric luminosities. All of these were calculated for the assumption that cluster spectra (with the exception of the Virgo cluster) could be well fit by isothermal bremsstrahlung.

3. PRE-HEAO CORRELATIONS AND INTERPRETATION

The large body of homogenous spectral data enabled one, for the first time, to correlate the detailed X-ray properties of clusters with their optical and radio properties. (The following discussion has been drawn from Mushotzky et al. 1978; Smith, Mushotzky and Serlemitsos 1979; and Mitchell et al. 1979).

In a thermal bremsstrahlung model the temperature of the X-ray gas is a measure of the cluster potential. A similar measure is the optical velocity dispersion of the galaxies. It was found that, for non-CD clusters, the X-ray temperature was proportional to the velocity dispersion squared. Treating the cluster sample together evidence was also found from this correlation that many clusters are nearly isothermal. This relationship between velocity dispersion and X-ray temperature strengthens the argument that clusters truly possess their virial mass; however the X-ray gas, with a mass similar to the optically luminous material, does not provide the missing mass.

Another strong correlation was found between the galaxy density in the core of the cluster, N_o, and the cluster temperature and emission integral. In fact it was found that KT was proportional to N_o which is expected if $KT \propto \Delta V^2$ and N_o is proportional to the true virial mass density. The correlation with emission integral along with a luminosity-temperature correlation indicated that high temperature clusters are, on the average, more centrally condensed or that they contain proportionally more intergalactic gas.

Correlations with the optical morphology of clusters and their member galaxies are also significant. (1) There appears to be a strong inverse correlation between the percentage of spirals in a cluster and the ram pressure experienced by an average galaxy in the cluster. This suggests that the remaining spirals in a cluster survive because they are too massive to be stripped by ram pressure. (2) There is a strong correlation between cluster spectral properties and their degree of central condensation as measured by Rood-Sastry or Bautz-Morgan type. The more central condensed clusters have, on the average, higher X-ray temperatures and higher emission integrals and therefore higher X-ray luminosities. This suggests that centrally optically condensed clusters have different X-ray properties (as has been recently shown for their X-ray morphology by Einstein results (see contribution by C. Jones this proceedings)).

4. HEAO 1 AND 2 SPECTRAL RESULTS

In this section I shall discuss the spectral results derived by the GSFC experiments on HEAO-1 and HEAO-2.

A. HEAO-1

HEAO-1 has observed $\sim$ 20 clusters in the 2-60 keV band with high counting statistics (see Fig. 1) and has detected Fe line emission in 18 of them. We now are beginning to see that there are small variations in the Fe abundance from cluster to cluster in the framework of an isothermal model. However one of the new discoveries from HEAO-1 is that many low luminosity clusters are <u>not</u> well discribed by an isothermal model. Before HEAO-1 we had only seen that for the Virgo cluster, now we have evidence (see Table 1) for $\sim$ 6 clusters that there probably exist at least 2 thermal components to their spectra.

The fact that this two-temperature structure is only seen in low L_X clusters by HEAO-1 may be related to the fact that only low L_X clusters show a complicated X-ray morphology (see C. Jones this volume). Unfortunately since we do not, with HEAO-1, have spatially resolved spectroscopy we cannot assign the Fe line to one component or the other thus making the Fe abundance, but <u>not</u> the equivalent widths, somewhat uncertain.

The vastly increased statistics available with HEAO-1 has also enabled us to detect the KB line of Fe. This transition

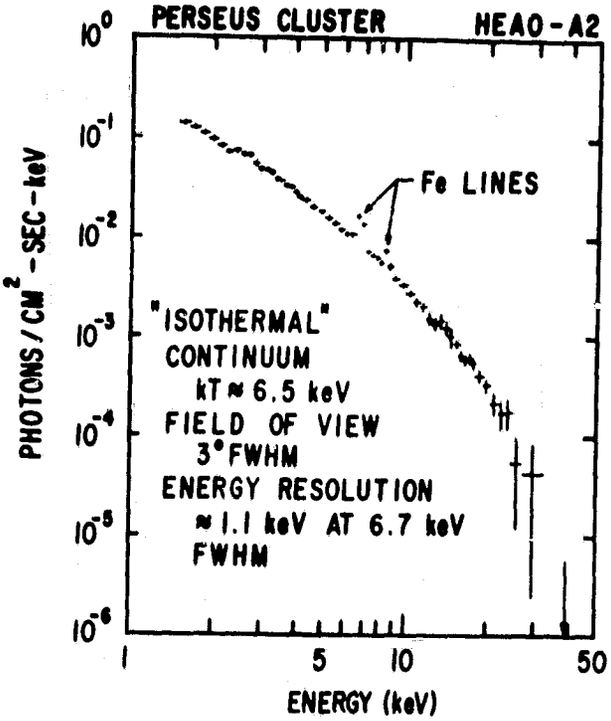

Fig. 1. The X-ray spectrum of the Perseus cluster as observed by HEAO-1 A-2. The line emission from the Kα and Kβ transitions of iron at 6.7 and 7.9 keV is quite prominent. Note also the unresolved line emission from 1.8 to 4 keV due to lines of Si, S, Ca and A.

proves that the line emission is not fluorescent but is truly due to recombination.

The extension of the number of very high quality spectra combined with the increase in the certainty of the cluster identification makes many of the correlations first described by OSO-8 and Ariel-5 data more certain. In Table 1 we show a summary of available spectral data for clusters. The HEAO-1 data are preliminary and the exact values should be used with caution.

B. HEAO-2

The solid state spectrometer (SSS) on HEAO-2 (Einstein) has an energy resolution of ∿ 160 eV (see contribution by S. Holt this volume) and a bandwidth from 0.8 to 4.0 keV. It is therefore capable of seeing recombination lines from the K shells of the lighter elements (such as Si, S and Mg) and from the L shell of Fe. Howeyer it cannot see the Kα and Kβ lines of Fe.

The SSS has detected lines due to Fe, Mg, Si and S in the X-ray spectrum of M87 (Fig. 2). For Si and S both the Hydrogenic and Helium lines have been seen. The line ratios are very sensitive to temperature, assuming collisional equilibrium, and a

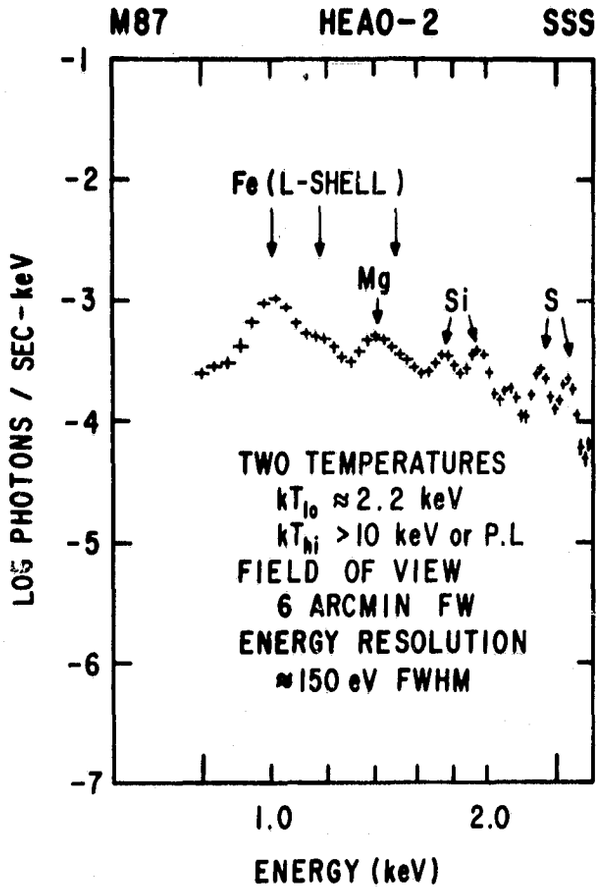

Fig. 2. The SSS spectrum of M87. Note the resolved line emission from both the hydrogenic and helium like lines of Si and S. The spectrum also displays line features due to Mg and the L shell transitions of Fe.

KT $\sim$ 1.8 keV is derived. The abundances of Si, S and Mg are approximately solar. We thus now know that as expected, elements other than Fe exist in the intragalactic cluster gas.

In the Perseus cluster the situation is more complicated. Here (Fig. 3) we also see lines due to both the Hydrogenic and Helium like lines of Si and S but the continuum gives a temperature such that one should only have the hydrogen-like lines. We interpret this to mean that there exists a very small amount of lower temperature gas (an amount small enough to escape detection by HEAO-1) in the core of the Perseus cluster and that this is evidence for cooling (as predicted by Cowie and Binney 1978) in the core of the cluster. The formal values derived from our observations give $\sim 10^{12}$ M$\odot$ of material to have cooled in a Hubble time and a cooling time of the low temperature material is less than $2\text{-}10^{9}$ yrs. Therefore, a substantial fraction of the mass of

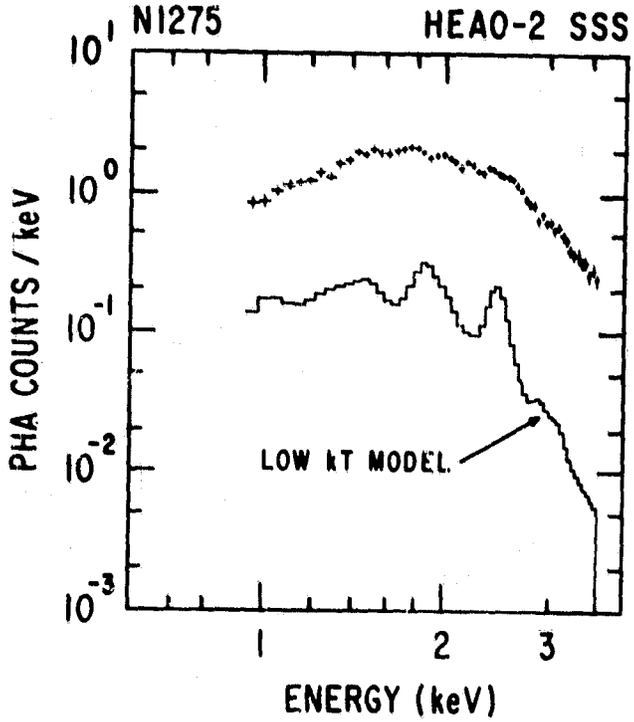

Fig. 3. The SSS spectrum of the core of the Perseus cluster. The solid line represents the best fit low temperature model which can account for the presence of the helium-like S and Si lines in the spectrum. This model has been correctly normalized to the total flux and shows the extreme sensitivity of a spectrometer to the presence of low temperature gas.

NGC 1275 is made up of material that has cooled and collapsed onto it from the intergalactic gas.

5. SUMMARY AND FUTURE

Spectral observations of clusters of galaxies have demonstrated that the X-ray emission is due to a hot evolved intracluster gas with $\sim$ 10% of the virial mass of the cluster. In low luminosity clusters there is an indication that there is thermal structure that may be related to the X-ray spatial structure. In the Perseus cluster there is evidence for cooling at the core and therefore for evolution of the cluster gas.

The X-ray gas is direct evidence for the existence of a virial mass in the cluster and responds to the cluster potential. This gas interacts with the galaxies in the cluster in a dynamic way and may change their morphology.

However, there are still many questions left. For example,

what is the temperature structure of the gas? Does there exist gradients in the elemental abundances across the cluster? What is the evolution of the elemental abundance of the gas with the age of the cluster? When and how does this gas arise?

Future observations, especially with spatially resolved spectroscopy and more sensitive X-ray telescopes may answer these questions.

ACKNOWLEDGMENTS

I thank B. Smith, P. Serlemitsos, E. Boldt and S. Holt for extensive discussion, encouragement, and their large contributions that have made this work possible.

REFERENCES

Catura, R.C., Fisher, P.G., Johnson, M.M., and Meyerott, A.J. 1972, Ap. J. 177, L1.
Cowie, L. and Binney, J. 1977, Ap. J. 215, 723.
Culhane, J.L. 1979 in IAU Symposium, ed. M.S. Longair and J. Einasto, Reidel (Boston).
DeYoung, D.S. 1978, Ap. J. 223, 47.
Gorenstein, P., Bjorkholm, P., Harris, B., and Harnden, F. 1973, Ap. J. 183, L57.
Gursky, H., Kellogg, E., Leong, C., Tananbaum, H., and Giacconi, R. 1971, Ap. J. 167, L81.
Kellogg, E. 1973, X-Ray and γ-Ray Astronomy IAU Symposium No. 55, ed. H. Bradt and R. Giacconi, Reidel (Boston).
Kellogg, E., Baldwin, J.R. and Koch, D. 1975, Ap. J. 199, 299.
Kellogg, E. and Murray, S. 1974, Ap. J. 193, L57.
Mitchell, R.J., Dickens, R.J., Bell, Burnell, S.S. and Culhane, J.L. 1979, M.N.R.A.S., in press.
Mushotzky, R.F., Serlemitsos, P.J., Smith, B.W., Boldt, E.A., and Holt, S.S. 1978, Ap. J. 225, 21.
Smith, B.W., Mushotzky, R.F., and Serlemitsos, P.J. 1979, Ap. J. 227, 37.

TABLE 1

NAME	kT_1	kT_2	6.7 keV E.W.	Fe/H	7.9 LINE?	OTHER LINES?	L_x^{44}	OBSERVATIONS*
A85	6.8±.5	No	300	1.2	?	?	6.7	4
A119	5.4±.5	?	300	0.95	?	?	3.7	1,4
A262	2.4±.8	?	?	?	?	?	0.38	1,2,4
NGC 1129 group	> 10	4.1±.3	630	1.8	Yes	?	2.0	2,4
A401	7.6±1.5	No	300	1.3	?	?	21.9	2,4
A426	6.4±.4	Very Weak	400	1.4	Yes	Si,S,Fe	12.4	1,2,3,4,5
0340-538	6.5±1.0	?	800	2.9	?	?	4.3	4
A478	7.3±1.0	No	360	1.5	?	?	22	2,3,4
Ser 40/6	9.0±.5	?	150	0.77	?	?	7.6	3,4
3C 129 cluster	5.4±1.0	?	330	1.0	?	?	2.7	2
0626-54	6.3±3	?	800	2.9	?	?	6.9	2,3
A754	11.0±3.0	No	< 150	< 1.0	?	?	10.4	4
A1060	> 10	2.0	800	2.5	?	?	0.17	2,4

Table 1 (continued)

A1367	2.8 ± 1.0	?	?	?	?	?	0.49	2
Virgo	> 10	2.2	1100	3.2	Yes	Mg,Si,S,Fe	0.29	1,2,4,5
Centaurus	8 ± 2	$2.4\pm.3$	600	> 1.4	Yes	?	0.71	1,2,3,4
A1656	$7.9\pm.3$	No	200	0.88	Yes	No ?	8.47	1,2,3,4,5
1326-311	$8.2^{+7.3}_{-3.0}$	?	?	?	?	?	12.0	2
A1795	5.8 ± 1.0	No	360	1.2	?	?	10.1	3.4
A2029	$6.2^{+2.6}_{-1.6}$	?	?	?	?	?	19.5	2
A2142	10.9 ± 1.0	No?	200	1.3	?	?	16.1	2,3,4
A2147	> 10	< 2	600	> 1.0	?	?	2.7	2,4
A2199	> 9	1.8	1000	> 3.3	?	?	2.8	2,4
A2256	7,+3,-2	?	?	?	?	?	8.2	2
A2319	12.5^{+7}_{-4}	?	?	?	?	?	12.7	2

*1 = Uhuru, 2 = OSO-8, 3 = Ariel 5, 4 = HEAO-1 A-2, 5 = HEAO-2 SSS